Geometry Optimization for Rotating Detonation Engines

a project presented to
The Faculty of the Department of Aerospace Engineering
San José State University

in partial fulfillment of the requirements for the degree
Master of Science in Aerospace Engineering

by

Sarah Hussain

May 2025

approved by

Dr. Yawo Ezunkpe
Faculty Advisor

ABSTRACT

Geometry Optimization for Rotating Detonation Engines

Sarah Hussain

Rotating detonation engines (RDEs) are gaining popularity for their potential to improve propulsion efficiency. This report investigates the performance of various RDE combustion chamber geometries, including annular, hollow, cone, and disk configurations in studies done worldwide. A comprehensive literature review and analysis of detonation wave theory laid the foundation for the study. Due to computational constraints, a simplified 2D ‘unrolled’ annular geometry was implemented in ANSYS Fluent, simulating multiple variations in size to examine the effect on thrust production. Hydrogen and air were selected as the fuel and oxidizer. The results were compared to Chapman-Jouguet (CJ) conditions to assess accuracy. By evaluating the impact of geometry on thrust production, this study provides insights into the performance of RDEs and their alignment with theoretical expectations.

ACKNOWLEDGEMENTS

I would like to acknowledge Dr. Yawo Ezunkpe for their guidance throughout this project. Special thanks to the researchers whose work on rotating detonation engines provided the foundation for this study.

TABLE OF CONTENTS

ABSTRACT iii
ACKNOWLEDGEMENTS iv
List of Figures vii
List of Tables ix
List of Symbols x
Chapter 1: Introduction 1
1.1 Introduction 1
1.2 Literature Review 2
1.2.1 First Theorized and Conceptualization of Detonation Waves from the 1950's 2
1.2.2 Most Recent Testing Done 3
1.2.3 Development Trends Observed in RDE's 5
1.2.4 University of Alabama Huntsville Racetrack Annular Geometry 5
1.2.5 Testing done at NASA Marshall Space Flight Center 6
1.2.6 Testing done at Air Force Institute of Technology 8
1.2.7 Testing Done with Multiple Geometric Configurations 9
1.2.7.1 Annular 9
1.2.7.2 Hollow 10
1.2.7.3 Disk 12
1.2.8 Testing done at NASA Glenn Research Center with a Disk RDE 14
1.2.9 Testing done in Poland 15
1.2.10 Testing done in Japan 16
1.2.11 Testing done in China 18
1.2.12 RDE Nozzle tests done using CFD 19
1.2.13 Testing done by the Naval Research Laboratory 20
1.2.14 U.S. Department of Energy CFD Combustion modeling of RDE 21
1.3 Comparative Analysis 22
1.4 Project Objective 24
1.5 Methodology 25
Chapter 2: Background, Theory, & Governing Equations 26
2.1 Historical Background & Foundational Experiments 26
2.2 Thermodynamic Principles 28
2.3 Detonation Wave Models 29
2.3.1 Deflagration vs Detonation 29
2.3.2 Rankine–Hugoniot Relations 30
2.3.3 CJ Theory 33
2.3.4 ZND Model 33
Chapter 3: Fuel & Oxidizer 36

3.1 Background Research..... 36
3.2 Thermodynamic Analysis of Multiple Mixtures.....36
3.3 NASA CEARUN Software.....37
Chapter 4: Research and Implementation of 2D model.....41
4.1 Literature review of 2 Dimensional RDE simulations.....42
4.1.1 Numerical Simulation of 2D Premixed Combustion Article.....42
4.1.2 Modeling 2D Linear Detonation Engines Article.....44
4.1.3 Simulation of Continuous Spin Detonation Article.....45
4.1.4 Examination of Wave Speed Using Simplified CFD Article.....47
4.1.5 2D Simulation of Detonation Wave Propagation in RDE Article..... 47
4.1.6 Feasibility and Performance with Ammonia/Hydrogen/Air Article.....49
4.1.7 Numerical Investigation of Species Transport Article.....50
4.1.8 Investigation of Detonation Theory and CRDE Article..... 51
4.1.9 Potential Scalability for Use in Non-Rocket Based Applications Article..... 53
4.2 2D Implementation on Numerical Setup..... 54
4.3 Comparative Analysis.....54
Chapter 5: Steps for Numerical Analysis & CFD Set-up..... 55
5.1 Simulation Framework.....55
5.2 Geometry Set-up and Mesh..... 55
5.3 Set up of Model.....56
5.4 Materials and Mixture.....57
5.5 Boundary Conditions..... 57
5.6 Ignition.....59
5.7 Method, Controls, & Initialization.....60
Chapter 6: Results and Discussion.....61
6.1 First Case..... 61
6.1.1 Pressure, Temperature, & Velocity Contours.....61
6.1.2 Analysis of Minimum and Maximum Values..... 62
6.1.3 Experimental CJ Parameters.....63
6.2 Results of Second Case.....65
6.2.1 Pressure, Temperature, and Velocity Contours.....65
6.2.2 Analysis of Minimum and Maximum Values..... 67
6.2.3. Experimental CJ Parameters.....68
6.3 Discussion.....70
6.4 Calculation Constraints and Performance Analysis Goals..... 71
Chapter 7: Conclusion and Future Work..... 72
References.....74
Appendix.....79

List of Figures

Figure 1.1 - Schematic diagram of cylindrical detonation chamber [1]..... 1
Figure 1.2 - Pratt & Whitney's RDE [6]..... 4
Figure 1.3 - VRD2 engine [9]..... 4
Figure 1.4 - Cross section of 4 inch racetrack RDE [11]..... 6
Figure 1.5 - Combustor dimensions [11]..... 6
Figure 1.6 - First geometric configuration of chamber assembly [3]..... 7
Figure 1.7 - Modular RDE cutaway sketch with critical variables [12]..... 9
Figure 1.8 - Schematic models of the (a) annular and (b) hollow geometry [14]..... 10
Figure 1.9 - Boundary and initial conditions of the numerical simulations [14]..... 11
Figure 1.10 - Schematic of the fuel injection surface [15]..... 11
Figure 1.11 - Pressure and temperature contours for cases 1-4 [15]..... 12
Figure 1.12 - Schematic diagram of annular RDC and disk-shaped RDC [16]..... 13
Figure 1.13 - Inward and outward geometric configurations of the RDE [17]..... 15
Figure 1.14 - Schematic diagram of cone shaped rocket geometry [18]..... 16
Figure 1.15 - Axial images of self-luminescence in the combustion chamber [19]..... 16
Figure 1.16 - Schematic cross section of RDE [19]..... 17
Figure 1.17 - Schematic of the throatless diverging RDE [20]..... 18
Figure 1.18 - Schematic of hollow and annular RDE [21]..... 18
Figure 1.19 - Schematic view of cylindrical chamber and the detonation wave structure [22].... 19
Figure 1.20 - Experimental test (a) and computational OpenNCC (b) temperature contour [23]. 20
Figure 1.21 - 3D pressure solution of the RDE [26]..... 21
Figure 1.22 - Temperature contour of unrolled geometry [26]..... 21
Figure 1.23 - Pressure and temperature contours for laminar and PaSR model [27]..... 22
Figure 2.1 - PDE testing set up [31]..... 27
Figure 2.2 - Spin detonation structure in a channel [32]..... 27
Figure 2.3 - Experimental set up for annular gap testing [5]..... 28
Figure 2.4 - Thermodynamic cycles of Humphrey's, Braytons, and Fickett-Jacob [33]..... 29
Figure 2.5 - Schematic representation of 1D combustion wave [29]..... 31
Figure 2.6 - Rayleigh line and Hugoniot curve [29]..... 32
Figure 2.7 - Schematic of ZND model [29]..... 34
Figure 3.1 - Input of results before CEA analysis [37]..... 38
Figure 4.1 - Unrolled annular geometry [1]..... 41
Figure 4.2 - Layout and direct ignition in RDE chamber [38]..... 43
Figure 4.3 - Initial conditions and domain composition [39]..... 45
Figure 4.4 - Temperature distribution and initiation regions [40]..... 46
Figure 4.5 - 3D to 2D conversion geometry [42]..... 48
Figure 4.6 - Regions and ignition strategy [42]..... 48

Figure 4.7 - Computational domain and boundary conditions [43].....50
Figure 4.8 - Input and output from combustion chamber [44]..... 51
Figure 4.9 - Patch sections for tube [45].....52
Figure 5.1 - Mesh.....56
Figure 5.2 - Species reactant mass fraction at inlet..... 58
Figure 5.3 - Species product mass fraction at outlet.....58
Figure 5.4 - Ignition zone.....60
Figure 6.1 - Pressure, temperature, and velocity contours in intervals of 20 time steps..... 62
Figure 6.2 - CJ Pressure plot.....63
Figure 6.3 - CJ Temperature plot..... 64
Figure 6.4 - CJ Velocity plot.....64
Figure 6.5 - Pressure, temperature, and velocity contour in intervals of 20 time steps.....67
Figure 6.6 - CJ Pressure plot.....68
Figure 6.7 - CJ Temperature plot..... 69
Figure 6.8 - CJ Velocity plot.....69

List of Tables

Table 1.1 - Simulation cases with different chamber sizes and fuel injection ratios [15].....11
Table 1.2 - Comparison of RDE geometries [13-15].....13
Table 3.1 - Fuel & oxidizer thermodynamics properties [35].....37
Table 3.2 - Initial conditions of unburned gas [37].....38
Table 3.3 - Detonation parameters [37].....39
Table 3.4 - Initial conditions of burned gas [37].....39
Table 3.5 - Mass fractions of burned gas [37].....40
Table 4.1 - Mass fraction for stoichiometric mixture of H2/Air [38].....43
Table 5.1 - Dimensions of geometric variations.....55
Table 6.1 - Minimum and maximum values recorded from contours.....63
Table 6.2 - Benchmark comparison to experimental data.....65
Table 6.3 - Minimum and maximum values recorded from contours.....68
Table 6.4 - Benchmark comparison to experimental data.....70

List of Symbols

Symbol	Definition	Units (SI)
a	Speed of Sound	m/s
d	Specific Volume	m^3/kg
E_a	Activation Energy	J/mol
F	Thrust	N
G	Gibbs Free Energy	kJ/kg
g_0	Gravity	m/s^2
h	Enthalpy	J/kg
I_{sp}	Specific Impulse	s
k	Pre-Exponential Factor	s^-1
M	Mach Number	------
ṁ	Mass Flow Rate	kg/s
M	Molar Mass	g/mol
p	Pressure	Pa
q	Heat Release	J/kg
R	Specific Gas Constant	J/kg·K
S	Entropy	kJ/kg·K
T	Temperature	K
u	Flow Field Velocity	m/s
U	Internal Energy	kJ/kg
V_{eq}	Equivalent Velocity	m/s
Greek Symbols		
ε	Epsilon	------
ɣ	Specific Heat Ratio	------
ρ	Density	kg/m^3
ω	Omega	rad/s
λ	Lambda	m
Subscripts		
$()_0$	Initial	------
$()_1$	State 1	------
$()_2$	State 2	------
$()_{CJ}$	Chapman-Jouguet	------
$()_e$	Exit	------
$()_{atm}$	Atmospheric	------
Acronyms		

2D	2 Dimensional	------
3D	3 Dimensional	------
CAD	Computer Aided Design	------
CFD	Computational Fluid Dynamics	------
CFL	Courant–Friedrichs–Lewy	
CJ	Chapman-Jouguet	------
CRDE	Continuous Rotating Detonation Engine	------
CSD	Continuous Spin Detonation	------
DARPA	Defense Advanced Research Projects Agency	------
DDT	Detonation to Deflagration Transition	------
DOD	Department of Defense	------
FRC	Finite Chemistry Model	------
ISAT	In-Situ Adaptive Tabulation	------
LES	Large Eddy Simulation	------
LPRE	Liquid-Propellant Rocket Engine	------
NASA CEA	NASA Chemical Equilibrium with Applications	------
NOx	Nitrogen Oxides	------
PaSR	Partially Stirred Reactor	------
QD2	Quasi 2D	------
RDE	Rotating Detonation Engine	------
RANS	Reynolds-Averaged Navier–Stokes	------
RHO	Density	Kg/m^3
SST	Shear Stress Transport	------
TCI	Turbulence-Chemistry Interaction	------
TVD	Total Variation Diminishing	------
UDF	User Defined Function	------
URANS	Unsteady Reynolds-Averaged Navier–Stokes	------
VDR2	Venus Detonation Ramjet	------
ZND	Zel'dovich-von Neumann-Döring	------
Chemical Species		

Ar	Argon	------
C2H4	Ethylene	------
C2H6	Ethane	------
C3H8	Propane	------
CH4	Methane	------
CO	Carbon Monoxide	------
CO2	Carbon Dioxide	------
H	Hydrogen Atom	------
H2	Hydrogen	------
H2O	Water	------
HO2	Hydroperoxyl Radical	------
N2	Nitrogen	------
NO	Nitric Oxide	------
NO2	Nitrogen Dioxide	------
O	Oxygen Atom	------
O2	Oxygen	------
OH	Hydroxyl	------

Chapter 1: Introduction

1.1 Introduction

Rotating detonation engines (RDEs) have gained significant attention in recent years offering some of the most advanced technological developments in the propulsion industry, providing an alternative to traditional rocket engines. The main distinguishing features lie in its unique, simple, yet compact design, as it has no moving parts, and method of generating thrust. Traditional rocket engines utilize deflagration, subsonic combustion, while RDE's use detonation, supersonic pressure gain combustion, achieving greater fuel efficiency, resulting in the ability to theoretically produce up to 25 percent more efficient thrust. An image of the geometric configuration of a typical RDE as well as the formation of the detonation front within the combustion chamber can be seen down below in Figure 1.1.

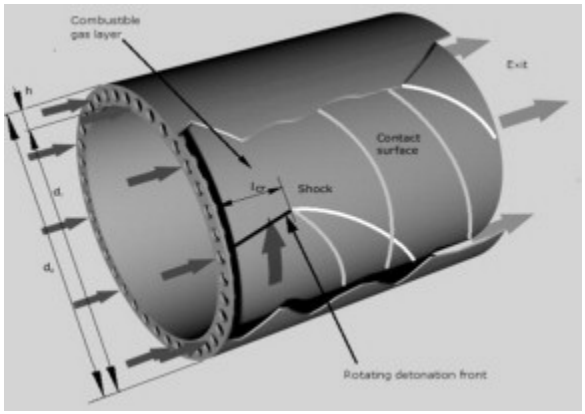

Figure 1.1 - Schematic diagram of cylindrical detonation chamber [1].

These new types of engines are going to play a vital role in the near future because as technology advances, so do deep space missions. Additionally, by wanting newer, faster, and more advanced aircrafts, such as fighter jets, missiles, or even supersonic aircrafts, an advancement in the type of engine is also required. For instance, the Air Force Research Laboratory is wanting to apply RDE's to many military applications such as air-to-ground weapons, air-to-air missiles, and surface weapons. The operational benefits they discuss consist of high performance in ratio to its compact size as well as being able to deliver better range, survivability, affordability, and even providing a credible threat to enemy systems [2]. Furthermore, they know that the utilization of RDE's can be employed in a wide range of engine configurations, some of which being ramjets, rockets, and even gas turbines [2].

These new types of engines will be able to provide the proper amount of power and thrust needed for mission completion. It is known that the current rocket engines still being used today will not be able to meet these requirements needed for the main production of thrust, efficient

fuel consumption, and overall performance. As many companies are continuing with trying to advance the current engines they have, some have begun switching over to heavily research RDE's as they know the potential of these engines. One example can be seen with the research and experimental testing done of a continuous rotating detonation engine at NASA Marshall Space Flight Center. Their research focused on the development of a continuous rotating detonation engine (CRDE) with the hopes of being able to apply it to future lander and interplanetary space exploration missions. They know that the performance benefits and compact geometry of the RDE will be better suited to be used for missions specifically to the Moon and then to Mars [3].

As this new technology is still in early stages of being researched and tested by many companies worldwide, there have been similarities in where rotating detonation engines are lacking and need further improvement. One of the main issues being the maximum optimization of the geometry setup, which directly affects their ability to maximize performance. The main trend seen from multiple companies that have performed experiments and tests are their size differences in their chamber size, outer diameter and channel width, as well as the type of geometry they are using. Majority of the testing done in the U.S. has stuck with either an annular or hollow geometry. However, international research has explored a broader range of configurations. For instance, in Japan, numerous institutions have conducted tests and experiments focusing on disk-shaped geometries, while in Poland, researchers have explored cone-shaped configurations.

1.2 Literature Review

The primary objective of this literature review is to research each institution that has done experiments on the different types of geometry of an RDE. Specifically, on why they chose it and how it benefited their results, and if it can be implemented on another experimental test to yield better results. The review will provide comprehensive background information which includes what their inspiration was to conduct the experiments, experimental setup such as picking the geometry, fuel, oxidizer, materials, etc, and the data gathered from their experimental results. A comparative analysis will be done to identify similarities and differences between them, specifically how their geometry set up yielded their results. Additionally, comparisons will be made to the type of fuel, oxidizer, and materials chosen, seeking patterns or insights across studies. This investigation will involve a detailed analysis of the theoretical and experimental studies work conducted by each company and institution.

1.2.1 First Theorized and Conceptualization of Detonation Waves from the 1950's

In the 1950's, Professor James Arthur Nicholls at the University of Michigan was one of the first people to theorize the use of detonation waves for the production of thrust. He built and tested

his theory with a pulse detonation engine and also worked on conceptualizing an engine that would be able to propagate a continuous rotating detonation [4]. However, there were many work limitations due to the time period, which is why there is now an increase in the researching and testing of this unique propulsion technology. During this time, there were other scientists around the world, also studying detonations as a new means to produce thrust. The tricky part was not causing an actual detonation and also being able to sustain a detonation wave.

Russian physicist Bogdan Voitsekhovsky was able to successfully describe the structure of spinning detonation waves, particularly their three-dimensional aspects in confined geometries [5]. He was also able to determine how transverse waves interact within detonation fronts, which contributed to the conceptual framework needed to stabilize rotating detonation waves in engines. Voitsekhovsky would also be one of the first to propose to utilize these rotating detonation waves for propulsion. His research began with different geometric configurations for the combustion chamber to determine if they could sustain detonation waves as well as looking into the different types of injection schemes.

Current experiments and studies done today on rotating detonation engines use Voitsekhovsky's work as it lays out the foundational framework required for understanding the dynamics of sustaining and propagating detonation waves, which will be further discussed in Chapter 2. This chapter will also cover the background, theory, and governing equation as well as where the Chapman-Jouguet, CJ theory, and the Zel'dovich-von Neumann-Döring model, ZND model, originated from. The next section will dive into the most recent successful testing done with rotating detonation engines, including a list of companies that also are currently investigating them.

1.2.2 Most Recent Testing Done

In March 2025, Pratt & Whitney announced the successful completion of a series of tests on its RDE, conducted in collaboration with the RTX Technology Research Center. Their main goal was to provide a new type of power generation for missiles being designed by Raytheon. The two main benefits they state is its simple design with no moving parts and the cost effective production while achieving a high thermal efficiency and performance. However, the two main challenges they faced were perfecting the fuel injection system and the design and manufacturing of parts for the new system. For the fuel injection system, the mixture and introduction of the fuel and oxidizer needed to be accurate and precise because it directly affects the ability to generate the detonation wave. For the design and manufacturing, they utilized additive manufacturing as it allowed for quick changes to be made in the design and the ability to use unusual specifications when crafting durable test articles [6]. Their next step is to keep advancing the design and manufacturing in order to hopefully conduct a test with the engine integrated with a ground vehicle. Specifications on the design, dimensions, fuel and oxidizer used were not published, but an image can be seen down below in Figure 1.2.

Figure 1.2 - Pratt & Whitney's RDE [6].

One major agency that is currently investigating RDE's is the Department of Defense's (DOD) Defense Advanced Research Projects Agency (DARPA). The specific program that they have dedicated to the development and testing of an RDE is called the Gambit program. Their main goal is to produce and test a preliminary design of the freejet test article and also to substantiate the design with an inlet and combustion for testing [7]. This program aims to establish the groundwork for the potential development of future prototype weapons.

Venus Aerospace, in partnership with DARPA, was able to successfully achieve a long duration engine test. The company's main goal is to provide a reusable hypersonic economy, for both commercial and defense purposes [8]. The three main benefits found were an increase in efficiency, a higher thrust-to-weight ratio, and reduced emissions. Another engine that they are currently working on is the Venus Detonation Ramjet (VDR2), which specifically combines the capabilities of a high thrust from an RDE and the cruise efficiency of a ramjet, in order to produce speeds up to mach 6 [9]. They were able to generate 2000 lbs of thrust with this engine. Some applications consist of dynamic space operations, airport to airport hyperlogistics, and low cost, high speed drones. An image of this engine can be seen down below in Figure 1.3.

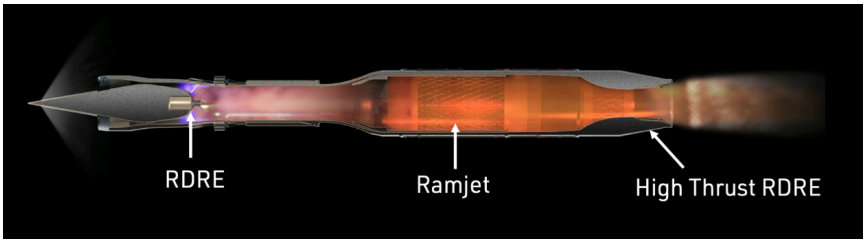

Figure 1.3 - VRD2 engine [9]

Rotating detonation engines are revolutionizing propulsion technology with their potential for greater efficiency and performance. As experimental research continues to validate their advantages, these engines are paving the way for advancements in aerospace and defense

applications. These are just a few of the companies that have successfully conducted experimental hot fire testing of an RDE. These next couple of sections will now cover both theoretical and experimental testing done by institutions all over the world. Specifically looking at how they conducted their experiments, components, geometric configurations they used, as well as the results obtained. The main goal at the end of this section, will be to provide a comparative analysis of the research done, consisting of the geometric configuration, dimensions, fuel and oxidizer, initial conditions, and the results yields.

1.2.3 Development Trends Observed in RDE's

One amazing article that was researched, analyzed the development trends of the experimental studies done on rotating detonation engines. They were able to conduct a clear and concise analysis on all the known RDE studies done worldwide and provided a performance comparison between them. They provided data on the engine type, geometry, chamber size, propellant, wave speed, and thrust for each institution in specific countries [10]. This made it very clear to see where exactly the data compares and contrasts on how these institutions conduct their experiments with RDE's. From looking at the tables provided in this article, it is very clear to see the different components used for each institution. This makes it very easy to determine which experiments need to be further investigated. For instance, when it comes to looking at the geometry, it is clear that most of the testing done in the U.S. has used annular geometry, same goes for Russia, France, and Germany. However, looking at Poland, specifically the Institute of Aviation, they tested three different types of geometry consisting of a cone, disk, and annular shape. This made it clear that studies and testing done worldwide needed to be further investigated.

From their analysis of the developmental trends, they determine 3 areas of improvements and for the ability to technologically advance the capabilities and performance of RDE's. These areas include geometry optimization of the combustors, injectors, and nozzles in order to maximize performance, combustion instability, and cooling. These areas need to be further researched and tested in order to obtain the most optimal RDE.

1.2.4 University of Alabama Huntsville Racetrack Annular Geometry

A study done by the Propulsion Research Center at the University of Alabama, conducted an experiment with a racetrack shaped combustion channel. Their main goal was to study the behavior of cyclically propagating detonation waves as well as obtaining a better understanding of the injection and combustion processes. For their experiment, they chose to use liquid propane and gaseous oxygen for their fuel and oxidizer. An image of the cross section can be seen down below as well. Looking at the dimensions of the combustion chamber, they went with choosing a 4 inch internal annulus diameter, 0.3 inch channel width, 0.066 inch throat gap, 4 inch combustor length, and a linear channel length of 4 inch. They were able to successfully design this unique

RDE and were able to get wave speeds from 975 to 1075 m/s. Additionally, they observed counter-propagating multi-wave detonating modes [11]. However, they discovered that with the use of liquid fuel, the engine was not able to stabilize into low-integer wave mode. The reason for this was not fully determined, however they do believe that it may have had something to do with either the chamber throat restriction, injection process, or the channel geometry. A key finding to note was that the behavior of the detonation wave relied on the mass flow rate and the equivalence ratio. They conducted their experiment with a mass flow rate between 0.277 to 0.640 kg/sec for the fuel mixture and also determined that an equivalence ratio between 1.75 to 1.8 obtained the highest detonation velocities [11]. This article is extremely beneficial as it provides the CAD drawings of the whole RDE, which means that the specific measurements and placement of all the components can be further investigated and help with obtaining a deeper understanding of the necessary background information required in designing an RDE with a slightly different geometry being used and the adaptations needed to be made for a successful test.

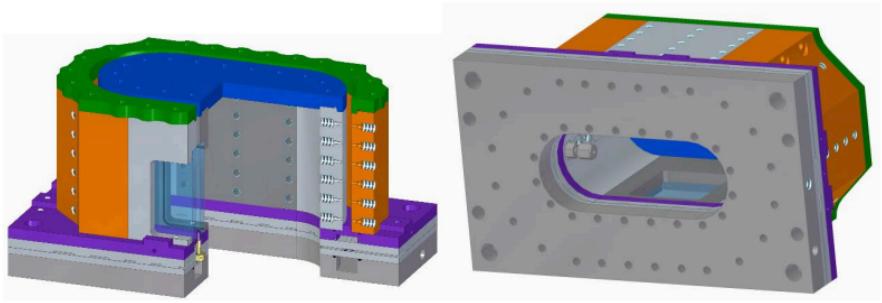

Figure 1.4 - Cross section of 4 inch racetrack RDE [11].

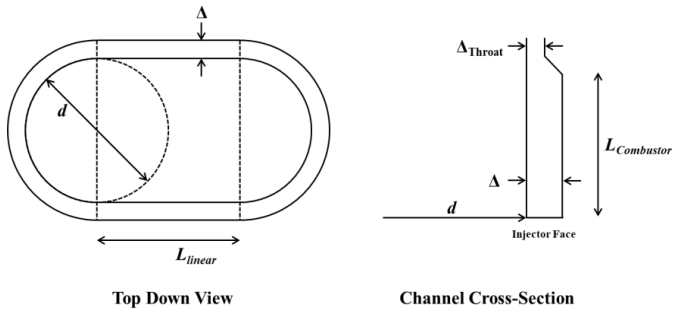

Figure 1.5 - Combustor dimensions [11].

1.2.5 Testing done at NASA Marshall Space Flight Center

One of the more recent experimental studies done on RDE's was done by NASA's Marshall Space Flight Center. Their main goal was to provide a detailed analysis on the technological

advancements they made regarding rotating detonation rocket engines along with what they were able to learn from the data gathered. One of the main ways they were able to achieve this was by integrating additive manufacturing and high performance copper base alloys, GRCop-42 and GRCop-84 [3]. They also went with testing two different geometric annular configurations of the chamber and using two types of propellant. Their first geometry consisted of a straight annular configuration, which had coolant channels running radially. It was designed to operate with deionized water or regenerative cooling with cryogenic liquid methane fuel [3]. The second chamber consisted of the same annular geometry but with integrated cooling channels running axially along with an integrated cowl extending to the exit plane of the plug nozzle [3].

The geometric configuration of the first geometry can be seen down below in Figure 1.6, however a CAD of the second geometric configuration was not provided. From the CAD, it is clear to see that the first geometric configuration of the chamber is comprised of 4 main components. However, the second configuration only consists of 2, an inner body with coupled contoured plug nozzle and an outer body with a coupled bell type outer nozzle [3]. The dimensions of their chamber geometry can be seen listed below [3].

- Overall length of 8.218 inches
- Inner body diameter of 5.59 inches
- Annulus gap width of 0.33 inches
- Expansion ratio of 5 inches
- Chamber volume/throat area of 2.9 inches
- 17.8 inches for volume from injector face to throat
- 2.736 inches for the length of the injector face to the throat

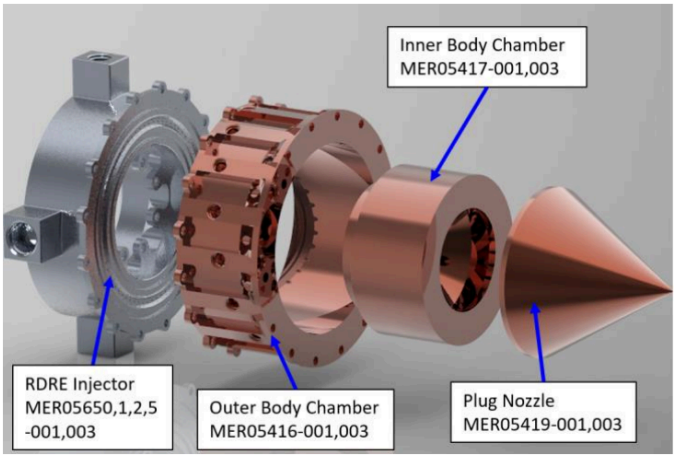

Figure 1.6 - First geometric configuration of chamber assembly [3].

Additionally, they also experimented with two types of propellant. The first type of propellant used was a combination of the liquid oxygen and gaseous hydrogen. The second type of propellant used liquid oxygen with both gaseous and liquid forms of methane. One of the main successful tests can be seen with the second geometric configuration along with the combined liquid oxygen gaseous methane propellant. This test was able to endure a chamber pressure of 622 psia and 4171 lbf of thrust, making it one of the most successful continuous rotating detonation rocket engines ever tested [3].

1.2.6 Testing done at Air Force Institute of Technology

The development and testing of a new 6 inch RDE done in 2012 by Jason C. Shank at the Air Force Institute of Technology, wanted to allow for multiple variations of injection and detonation channel widths [12]. For their fuel and oxidizer they went with hydrogen and standard air. Their design began with a simple detonation channel, with placement of the reactants plenums to the side and bottom of the channel, and making sure the orientation of the fuel and oxidizer would provide a homogeneous mixture in the detonation channel [12].

Additionally, they wanted their design of the RDE to have five critical variables be easily changeable. These five critical variables are the oxidizer type, oxidizer injection geometry, fuel type, fuel injection geometry, and the detonation channel [12]. By allowing for these five critical variables to be interchangeable, this will help with ease of adjustments in order to determine the best configuration if you want to test multiple variation setup of the RDE. With this ability in hand, one could perform multiple experiments and provide a comparative analysis to determine the best geometric configuration of the RDE.

The layout and dimensions can be seen down below[12]. From their experiment, they were able to obtain detonation wave speeds of 1410 m/s to 1560 m/s.

- 5.46 inch outer diameter
- Detonation channel of 0.3 inches
- Fuel plate thickness of 0.5 inches
- Spacer height of 0.125 inches
- 80 0.1 inch diameter holes on the fuel plate
- Arranged in a 5.96 inch diameter circle

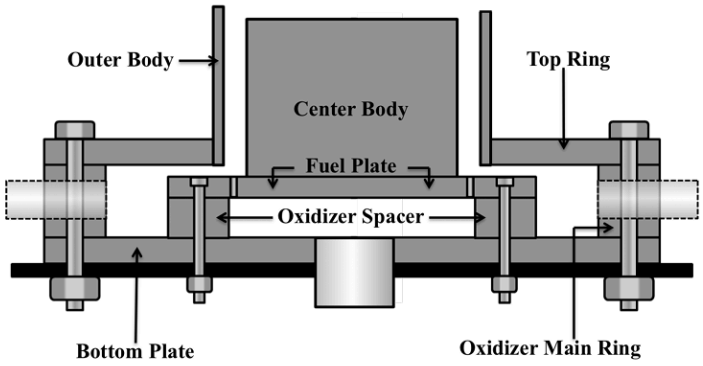

Figure 1.7 - Modular RDE cutaway sketch with critical variables [12].

1.2.7 Testing Done with Multiple Geometric Configurations

Researchers at the University of Cincinnati conducted an investigation on physics of rotating detonation combustor operations done worldwide and took note of the parallel challenges many have faced. This article dived into the structures and dynamics of an RDE, geometries, injection, fuel and oxidizers tested, combustion instabilities and more. When looking at the geometries, they specifically looked at annular, hollow, and disk. They provide in depth analysis of the geometries used, as well as the benefits and challenges faced. In order to provide a clear distinction of the benefits and challenges of each geometry, the information already gathered from this article can be seen down below in Table 1.2. Additionally, during their comprehensive investigation, they found that a fuel and oxidizer mixture of hydrogen and air were the most frequently used because of the ease in detonation of the mixture [13].

1.2.7.1 Annular

The first geometry that was investigated was annular. They researched multiple articles that used an annular geometry, but that had different dimensions such as channel width, length, as well as the inner and outer radius. From their investigation, it is clear that these geometric parameters play a huge role in the production and sustainment of detonation waves. Specifically, for the channel width, the larger the channel, the weaker the detonation wave front will be. However, another study that was conducted found that if the channel width is kept constant, but the diameter is increased, strong shock trains are produced and propagated downstream of the detonation wave [13]. Another study that was researched was found to have similar results, however, the length was changed while the diameter and width were both fixed. With these findings, they have determined that more research needs to be done on the rotating detonation combustor flow field with three dimensionality.

Another study showed that having a large diameter and a large annulus width helps with highly stable rotating detonation combustion operations, however it is important to keep in mind that

the larger widths and diameters will likely lower the overall mass flux through the annulus. This will cause lower fill heights of the mixture upstream of the wave, which in turn can make the combustor susceptible to an unstable operation [13]. It is clear that there are many tradeoffs when it comes to the specific size of these geometric parameters.

1.2.7.2 Hollow

When looking at a hollow geometry, the physics hold true with some additional geometric parameters. One of the first notable differences between a hollow and annular geometry is the removal of the inner wall. One study they mentioned conducted a three dimensional numerical investigation of an RDE with a hollow combustor. Their main goal was to provide an alternative to co-axial annular RDE's as they had the tendency for the engine overheating [14]. The results obtained from their numerical solution conclude that detonation waves can indeed be sustained and propagate due to the evidence of no repeated reflection of the detonation waves, however without the inner wall, there is a tendency for the fresh gas mixture to compile and cause non detonation burning. They also found that there is lower kinetic energy proportion in the axial direction and as well as the burnt gases were exhibiting a slightly more divergent flow [14].

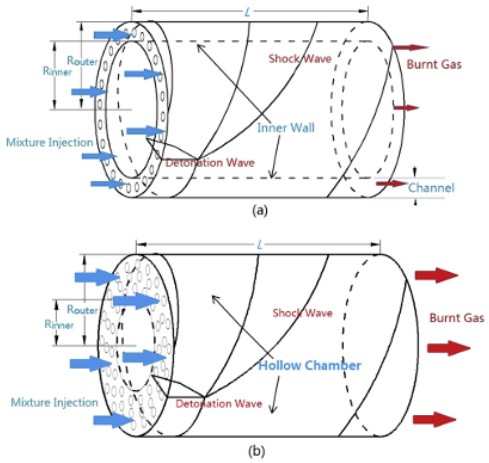

Figure 1.8 - Schematic models of the (a) annular and (b) hollow geometry [14].

Additionally, this article also provides the numerical framework it used for their three dimensional simulations, which consists of the governing equations, boundary and initial conditions as seen in Figure 1.9. This provides a better understanding of the process of conducting a three dimensional simulation of an RDE.

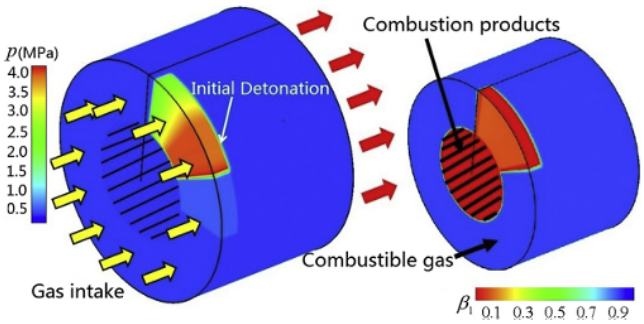

Figure 1.9 - Boundary and initial conditions of the numerical simulations [14].

Another article also investigated performing a three dimensional numerical study of a hollow RDE. Their main goal was to study different fuel injection, flow fields, and the propulsive performances to see whether they were a better option compared to RDE's with an annular geometry [15]. They conducted four simulations with different chamber sizes and fuel injection ratios. The schematic and the table of the varying ratio and dimensions can be seen down below. It was determined that the fuel injection area ratio did indeed play a critical role in the flow field of the hollow RDE, and the removal of the inner wall did affect the fuel injection condition [15]. Specifically, when comparing the hollow RDE to the annular RDE, they found that velocity of the fuel flow on the injection is greater.

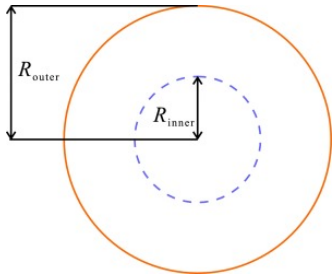

Figure 1.10 - Schematic of the fuel injection surface [15].

Table 1.1 - Simulation cases with different chamber sizes and fuel injection ratios [15].

	R_{inner}	R_{outer}	ψ
Case 1	2cm	5cm	84.0%
Case 2	2cm	6cm	88.9%
Case 3	3cm	6cm	75.0%
Case 4	4cm	6cm	55.6%

For their CFD analysis, they gathered data on the pressure and temperature contours for all four cases. In figure a, two detonation wave fronts can be seen propagating toward each other. This causes the detonation velocity to fluctuate, making it unstable. However, in the rest of the cases, dynamic stability is reached, detonation velocity approaches the CJ velocity, and the multiple

stationary detonation waves can be observed. The detonation waves front are also observed to be curved in the radial direction. From this simulation, they determined that the smaller the outer radius is for a hollow combustor, the more time it takes to reach a stable state.

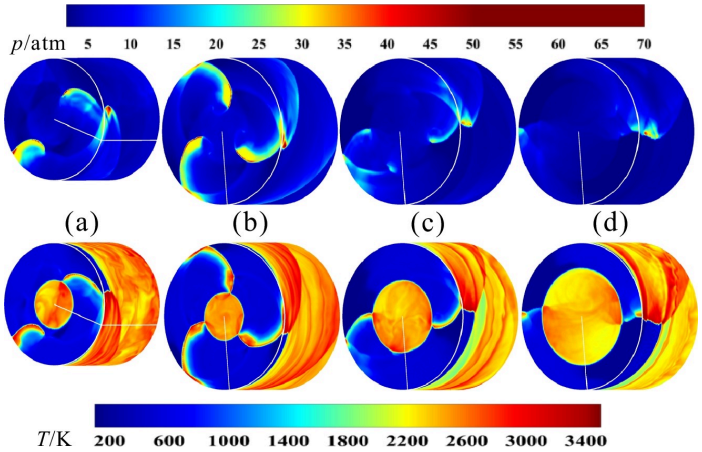

Figure 1.11 - Pressure and temperature contours for cases 1-4 [15].

1.2.7.3 Disk

Looking at the disk shaped RDE, there are some clear notable differences when comparing it to the annular and hollow geometries as discussed prior. The main difference can be seen with the reactants being fed radially inward or outward. A study done by Nagoya University, Keio University, and Japan Aerospace Exploration Agency consisted of the investigation of a disk shaped combustor, as it may provide a higher combustion chamber pressure than the traditional annular ones [16]. A comparison of both geometric configurations can be seen down below in figure 1.13. The dimensions of the combustion chamber were 5 mm wide with an outer diameter of 130 mm and an inner diameter of 75 mm. For their fuel and oxidizer, they used ethylene and oxygen.

From their experiment, they were able to observe forward facing detonation waves, both propagating clockwise and counterclockwise, with a combustion chamber static pressure of around 90 percent of the fuel and oxidizer plenum pressure [16]. They also noticed that the detonation waves were able to intersect and pass through each other and not lose their shape. However the velocity measured wasn't close enough to their CJ velocity. They determined that this could have been due to inadequate mixing of propellant, which can also cause the shape of the leading shock wave to become distorted. The presence of burned gas within the detonation front medium as well as the discrepancies between the actual and true wave propagation directions were also noted [16].

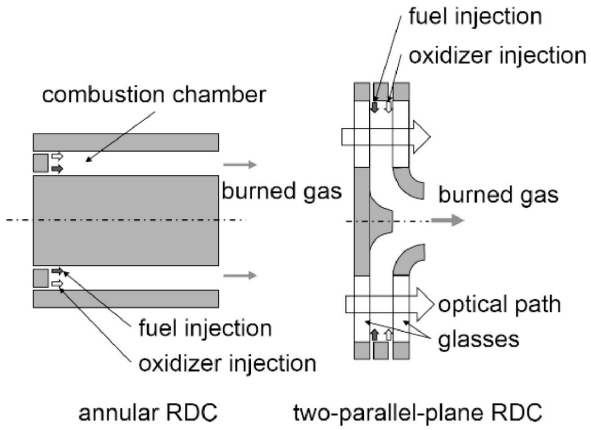

Figure 1.12 - Schematic diagram of annular RDC and disk-shaped RDC [16].

Table 1.2 - Comparison of RDE geometries [13-15].

Geometry	Pros	Cons
Annular	- Stable detonation wave propagation with optimized parameters. - Strong shock trains when the diameter increases while maintaining a constant channel width. - Well-researched and widely used.	- Larger channel width weakens the detonation wave front. - Increased annulus width and diameter can lower mass flux, leading to reduced fill height and potential instability.
Hollow	- Eliminates inner wall, reducing overheating issues common in co-axial annular RDEs. - Sustains detonation waves without repeated wave reflections. - Higher fuel injection velocity compared to annular RDEs.	- Fresh gas mixture tends to accumulate, causing non-detonative combustion. - Lower kinetic energy in the axial direction. - Burnt gases exhibit a more divergent flow, affecting efficiency.
Disk	- Can achieve higher combustion chamber pressures compared to annular designs. - Allows for both radially inward and outward reactant injection. - Detonation waves can intersect without losing shape.	- Potential for inadequate propellant mixing, affecting detonation efficiency. - Wave propagation direction discrepancies can distort the shock wave structure. - Experimentally less explored compared to annular and hollow configurations.

1.2.8 Testing done at NASA Glenn Research Center with a Disk RDE

A study done at NASA Glenn Research Center by Daniel E. Paxson consisted of a quasi two dimensional CFD simulation of a disk shaped RDE in order to investigate how this type of configuration affects its performance. The three geometric configurations simulated and compared were annular, inward, and outward. For their first configuration, the cross sectional area was held constant with inlet to channel ratio of 1, inner to outer diameter ratio of 0.4, and a length of 0.136. The results obtained from the simulation showed that a full detonation was observed with no fuel mixing spillage that resulted in a choked flow [17]. They also found that this configuration for both inward and outward was deemed unstable. However, for their second configuration, they used an inlet to channel ratio of 0.6, same inner to outer diameter ratio and length, and found that it was indeed stable. The third configuration was the same as the second but with an inner to outer diameter ratio of 0.3. Their results concluded that the annular shaped RDE had the best performance when compared to the inward and outward configuration. The annular model showed a 3 percent decrease, 11 percent decrease for the outward model, and 24 percent for the inward model as the radial length was increased.

The conclusion made was that as the size of the diameter ratio is reduced, the performance of both the inward and outward configurations suffer as a result. The last test performed consisted of an inlet restriction of 0.6, an inner to outer diameter of 0.4, as well as having the cross sectional area from the inlet to the exit diameter being reduced linearly by 30 percent [17]. They were able to confirm that the pressure gain increased by 52 percent and that both the inward configuration outperformed the outward and annular one.

The article is extremely beneficial as it provides an in-depth insight on the governing equations, initial conditions used, changing parameters, and how they utilized CFD and code. For instance, their simulations set up consisted of a semi-idealized mode such that it was adiabatic, inviscid, as well as not allowing backflow at the inlet to occur [17]. For their fuel and oxidizer ratio, they used stoichiometric hydrogen and air and also provided the adequate parameters, which can be seen listed below [17].

- Specific heat ratio - 1.264
- Real gas constant - 73.92 ft-lb_f/lb_m/R
- Fuel heating value - 51,571 BTU/lb_m

For their code, they don’t specify which type of code they're using, but they do include what was integrated into it. The code is a high resolution algorithm with quasi-two-dimensional, two-species, and reactive Euler equations with source terms on a regular Cartesian grid [17]. Since the simulation is non-dimensional, the specific parameters are given down below [17].

- Pressure - 14.7 psia
- Density - 0.055 lb_m/ft^3
- Temperature - 520 R
- Speed of sound - 1250 ft/s

Additionally, they also used an explicit, second-order, two-step, Runge-Kutta technique to integrate the governing equations numerically in time. [17] These steps and parameters chosen are very important to understand the implementation into CFD.

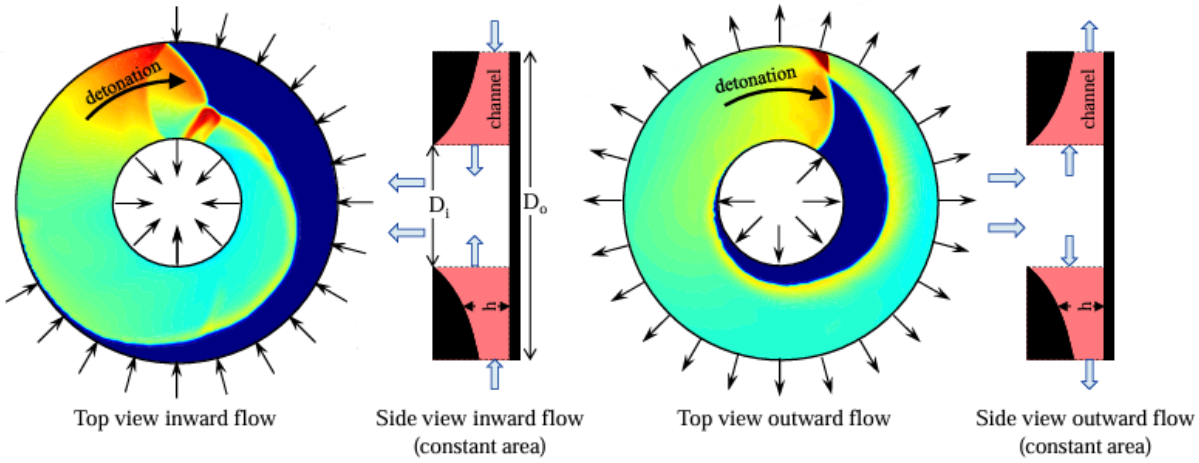

Figure 1.13 - Inward and outward geometric configurations of the RDE [17].

1.2.9 Testing done in Poland

The Institution of Aviation in Poland was able to conduct experimental testing of continuous rotating detonation engines. They also wanted to research different engine geometries and what conditions the engines needed for stability. They tested an annular, disk, and cone shaped chamber, however the dimensions for these were not given. For their fuel and oxidizer, they chose liquid nitrous oxide and liquid propane. From their results, they concluded that the cone shaped chamber was able to deliver the biggest specific impulse, between 250-270 N for 200 seconds [18]. They were able to confirm these results with theoretical calculations from NASA's CEA Code with 95 percent accuracy. They then went forward and designed the engine to be attached to a rocket. The rocket was able to reach an altitude of 500 meters.

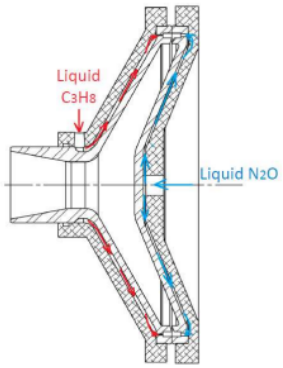

Figure 1.14 - Schematic diagram of cone shaped rocket geometry [18].

1.2.10 Testing done in Japan

Experimental studies done by Nagoya University, Keio University, and the Japan Aerospace Exploration Agency, were specifically looking at varying inner cylinder radius for an RDE and how they affect the thrust. The type of propellant used was gaseous ethylene and gaseous oxygen. Dimensions of their experimental set up can be seen listed below and in the figure.

- Length of chamber - 70 mm
- Outer radius - 39 mm
- Varying inner radius - 31 mm, 23 mm, 15 mm, 9 mm, 0 mm

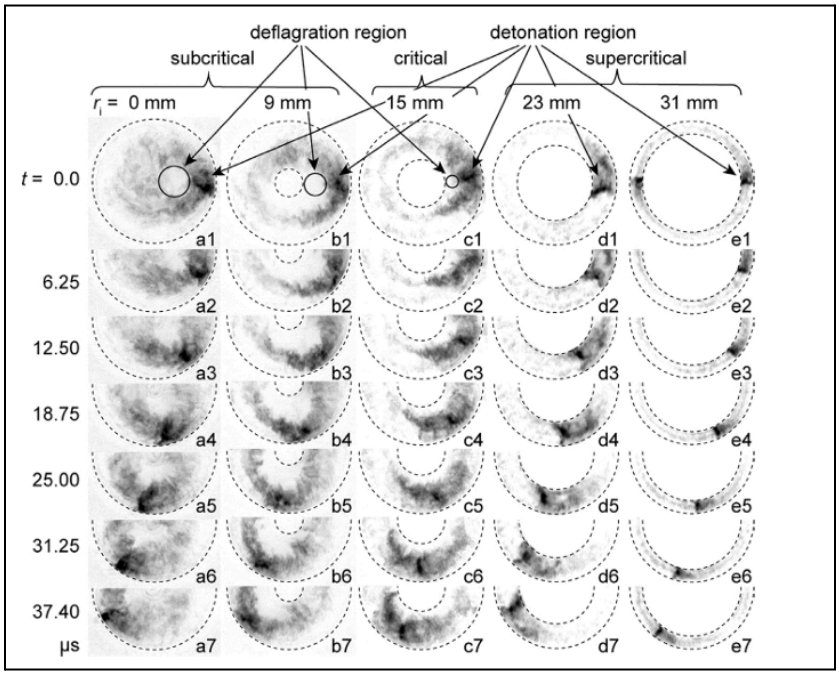

Figure 1.15 - Axial images of self-luminescence in the combustion chamber [19].

Their experimental results concluded that a radius of 15 mm was best for adequate thrust generation as it was close to the critical conditions for sustaining detonation waves [19]. They conducted the experiment with specific ranges for the mass flow rate and equivalence ratio. Specifically for the radius of 15 mm, the mass flow rate was 132 ± 13 g/s and an equivalence ratio of 1.01 ± 0.1. The results can be seen listed below [19].

- Combustion chamber pressure - 48 ± 3 kPa
- Thrust - 251 ± 13 N
- Specific impulse - 194 ± 19 s
- One detonation wave
- Detonation frequency - 8.6 ± 0.3 kHz
- Detonation velocity - 1900 ± 50 m/s

The schematic diagram of the RDE and where the radius is changing as well as the dimensions can be seen down below in Figure 1.16.

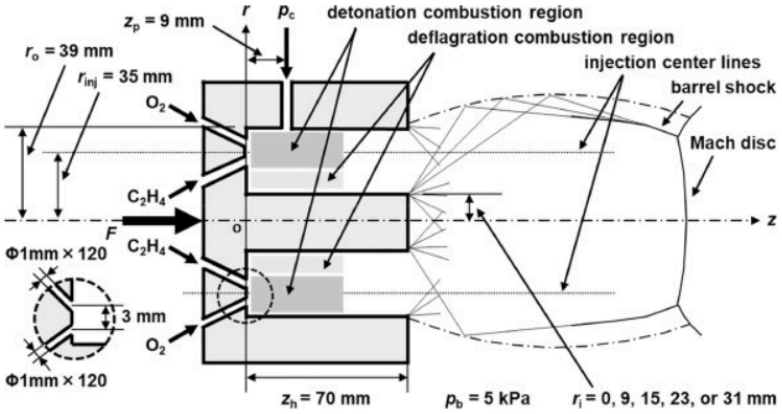

Figure 1.16 - Schematic cross section of RDE [19].

An experimental investigation done by Nagoya University, Keio University, Japan Aerospace Exploration Agency, and Purdue University looked into the inner flow of a throatless diverging rotating detonation engine with two types of ignition methods [20]. They tested it with a deflagration to detonation transition (DDT) and a direct ignition. The dimensions of their RDE consisted of an inlet diameter of 20mm, engine length of 70 mm, and a 5 degree diverging angle. They chose a fuel and oxidizer of gaseous ethylene and oxygen. One interesting finding that they were able to determine was that the inner flow can be treated as a quasi one dimensional steady flow according to their experimental and calculated results [20]. They measured the flow velocity to be 1261 m/s.

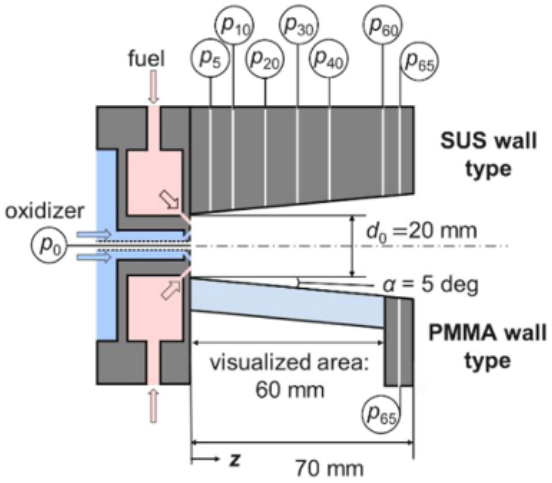

Figure 1.17 - Schematic of the throatless diverging RDE [20].

1.2.11 Testing done in China

Experimental research done at Peking University was able to conduct an investigation on the performance between a hollow and annular RDE with nozzles. They tested a total of four configurations with gaseous methane and gaseous oxygen as their propellant. They had a mass flow rate in the range of 50 and 300 g/s and an equivalence ratio between 0.3 and 1.5. The results revealed that the hollow chamber outperformed the annular geometry in terms of injection pressure loss, despite having a slightly lower characteristic velocity efficiency, averaging between 0.7 and 0.79 for the hollow chamber and 0.75 to 0.8 for the annular configuration [21].

One notable finding was that the Laval nozzle significantly outperformed the aerospike nozzle, which was unexpected given the widespread belief in the efficiency of aerospike designs [21]. This study highlights the potential of exploring alternative geometric and nozzle configurations in RDEs, providing valuable insights for future design optimization. The figure below provides the schematic representation of both geometries and the varying dimensions.

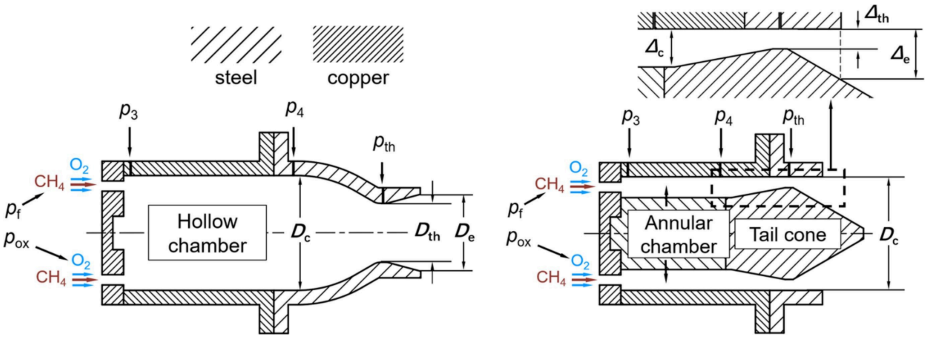

Figure 1.18 - Schematic of hollow and annular RDE [21].

The National University of Defense Technology in China, conducted an investigation where their research focused on an RDE with a hollow combustion chamber along with gaseous methane and oxygen being utilized as their fuel and oxidizer. The dimensions of the RDE consisted of a sleeve diameter of 100 mm, and a length of 75 mm. The injection pressures for the fuel and oxidizer injection manifolds were 0.577 MPa and 0.711 MPa, with an average mass flow rate of 217.2 gs^-1 for oxygen and 36.1 gs^-1 for methane, and an equivalence ratio of 0.665 [22]. They were able to determine that it was indeed feasible to sustain a continuous rotating detonation wave in a hollow combustion chamber through annular injection distribution as they were able to obtain an average frequency of 19.251 kHz and velocity of 1512 m/s [22]. The schematic view below provides a visual representation of the chamber as well as the formation of the detonation wave structure.

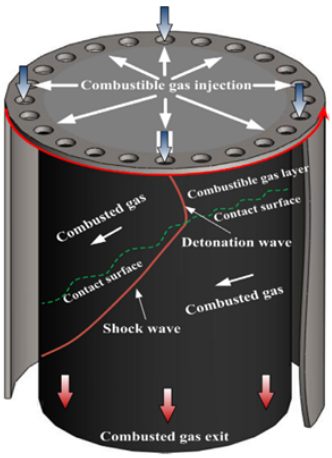

Figure 1.19 - Schematic view of cylindrical chamber and the detonation wave structure [22].

1.2.12 RDE Nozzle tests done using CFD

A numerical investigation at NASA Glenn Research Center took multiple RDE nozzle designs and conducted computational experiments to determine which one provided the most optimal performance. They began with a quasi-2D CFD code for an unsteady inflow generation and used data from research done at the Naval Postgraduate School to provide a validation for the geometry they obtained, converted the data, and used OpenNCC for the design optimization [23]. They used a fuel and oxidizer of methane and air. To reduce the amount of computational time, they found that by replacing the chemical kinetics calculation with a simple one-step heat release model, would do the trick. This was also referred to as the simplified in-house quasi-2D code, (QD2) [24]. They included their initial set up for their CFD and the QD2, however, the operating conditions can be seen listed below [23].

- Inlet pressure of 131.7 psia,
- Inlet temperature of 510 R
- Exit pressure of 14.7 psia

- Fuel/air ratio of 0.972
- Air mass flow rate of 1.51 kg/s

The QD2 begins with a single species, premixed, calorically perfect gas, and solving the Euler equations [25]. They also included that the "governing equations are integrated numerically in time, using an explicit, second-order, two-step, Runge-Kutta technique" [23]. This study is really interesting because of how they laid out their framework to conduct the experiments as well as what software they used. They provide extensive information on their theoretical analysis as well as how they achieved it. The capabilities of OpenNCC can be seen down below, when compared to the experimental test.

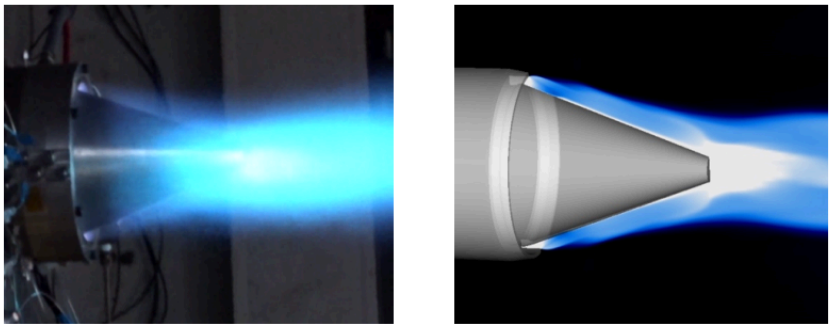

(a) Experiment (b) OpenNCC

Figure 1.20 - Experimental test (a) and computational OpenNCC (b) temperature contour [23]

1.2.13 Testing done by the Naval Research Laboratory

The Naval Research Laboratory conducted an investigation into the physics of a three-dimensional hydrogen-air based RDE, focusing on the flow field and its impact on key parameters, such as stagnation conditions. The dimensions consisted of an inner diameter of 13 cm, outer diameter of 15 cm, length of 17.7 cm, and a radius to thickness is 7. A key observation from this study was the simplification done by converting the 3D geometry into a 2D unrolled rectangular configuration, which reduced computational costs while retaining the ability to accurately capture detonation wave dynamics. This study is very important as it was able to demonstrate practicality of using a simplified 2D simulation to model complex 3D behaviors.

This approach not only demonstrated the feasibility of the 2D modeling but also laid the groundwork for further exploration into how 2D simulations can effectively replicate 3D detonation behavior, providing valuable insights into the potential benefits of such simplification. This concept will be further researched to establish a clear understanding of its principles and to develop a practical guide for implementing it effectively in future simulations. Figure 1.22 provides the temperature contour of the 2D unrolled geometry, as well as the detonation wave structure.

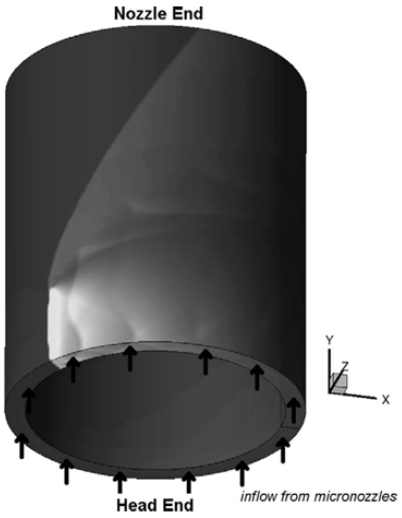

Figure 1.21 - 3D pressure solution of the RDE [26].

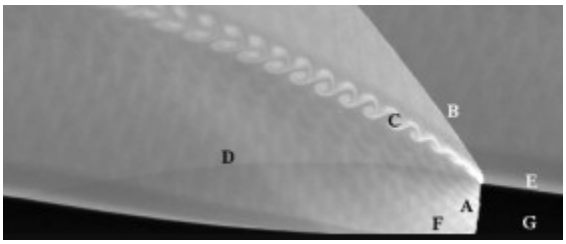

Figure 1.22 - Temperature contour of unrolled geometry [26].

1.2.14 U.S. Department of Energy CFD Combustion modeling of RDE

In this article, the U.S Department of Energy's main objective was to conduct CFD simulations on a rotating detonation engine using a zero-dimensional Partially Stirred Reactor (PaSR) model, a detailed hydrogen-air chemical kinetic mechanism, and examining the effects of mesh resolution on solution accuracy using the Large Eddy Simulation (LES) approach [27]. The data obtained from the simulation would then be compared to the experimental data. For their simulation, they used ANSYS Fluent 19.2 with an implicit pressure based solver. For the mesh around the inlet manifold and injector region, they used a hybrid mesh consisting of polyhedral cells, while using structured hexahedral cells for the annulus. The geometry consisted of an outer diameter of 154 mm, an inner diameter of 139 mm, and a length of 100 mm, with an air injection slot height of 1.78 mm and a fuel injector diameter of 0.89 mm [27].

The initial conditions for their 3D setup are presented as [27]:

- Temperature: 300 K
- Air flow rate: 0.6125 kg/s
- Fuel flow rate 0.01746 kg/s
- Equivalence ratio: 1

For their 3D simulations, they conducted multiple tests with and without the combustion model to determine the effect on the results. The first test consisted of the laminar model with a wave speed of 1790 m/s with a two wave solution. The second test had the PaSR model with an average wave speed of 1844 m/s and a single wave solution. When comparing this data to the experimental data provided by the Air Force Research Laboratory, they presented a single wave solution with a wave speed of 1740 m/s [27]. The second test was confirmed to be more accurate. The pressure and temperature contours of both tests can be seen down below in figure 1.23.

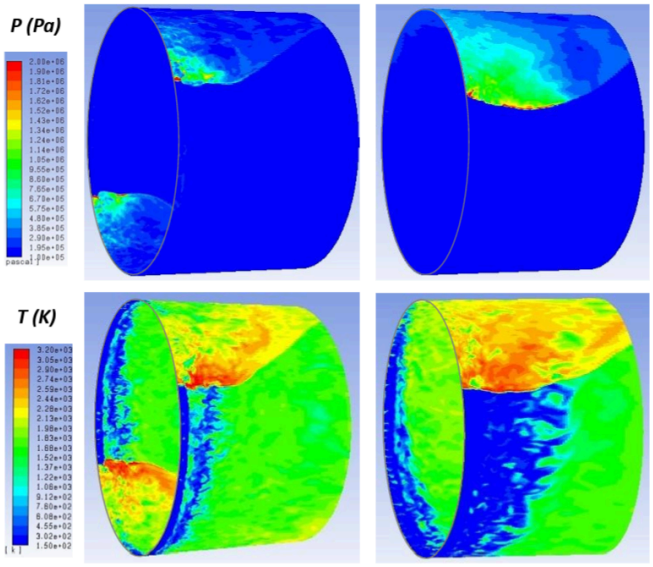

Figure 1.23 - Pressure and temperature contours for laminar and PaSR model [27].

This article is specifically beneficial as it uses the same software that this project requires, which is why extensive research was done on it. It lays of fundamental framework and understanding required to utilize Ansys Fluent for 3D simulations of RDE's.

1.3 Comparative Analysis

With the comprehensive literature review complete, the next step is to conduct a comparative analysis, reviewing the most notable experimental and computational studies on RDEs, focusing on their geometric configurations, propellant choices, and testing methodologies. The primary goal is to understand how these factors influence performance metrics. This analysis will provide a deeper understanding of the experimental and numerical testing conducted on RDEs, including the specific components and aspects being tested, the rationale behind these tests, the results obtained, and the similarities and differences in their setups. This approach will help identify

common trends, best practices, and potential areas for improvement in RDE design and performance evaluation.

1. Geometry and Design Configurations

A significant variety of RDE geometries have been investigated across multiple research institutions worldwide, including annular, hollow, disk, cone, and even racetrack-shaped configurations. In the United States, studies at NASA and the Air Force Institute of Technology mainly focused on annular and hollow designs, examining their ability to maintain stable detonation waves. Notably, NASA also explored disk-shaped RDEs, while the University of Alabama tested a unique racetrack-shaped configuration, adding to the diversity of geometries studied. Furthermore, there have been studies dedicated to optimizing RDE nozzle configurations to enhance performance.

In contrast, research institutions in China, Japan, and Poland have explored a broader range of geometric configurations, including hollow, cone, and disk-shaped RDEs. These studies have placed a strong emphasis on understanding how changes in geometry directly affect detonation wave stability, propagation speed, thrust generation, and overall performance. For instance, China has extensively investigated hollow and annular designs, Japan has focused on disk-shaped configurations and varying sizes of a hollow chamber, and Poland has explored cone-shaped chambers. This diverse exploration highlights the global effort to determine the most efficient and effective RDE geometries for various applications.

2. Propellant Selection

Hydrogen and air were the most commonly used propellants in the reviewed studies, particularly for their high reactivity and well-understood detonation characteristics. The choice of fuel-oxidizer pairs was directly tied to the study's objectives, with hydrogen-air being favored for studies aiming to maximize detonation wave speeds, while methane-oxygen was used to explore efficiency and stability.

3. Testing Methodologies: Experimental vs. Numerical

The studies employed both experimental and numerical approaches, each with distinct advantages. Experimental tests, such as those conducted by NASA, provided direct measurements of thrust, wave speed, and stability but were limited by cost, safety concerns, and complexity. Numerical studies, such as the CFD simulations at NASA Glenn and the U.S. Department of Energy, enabled detailed analysis of flow fields, wave structures, and performance metrics without the constraints of physical testing. The Naval Research Laboratory highlighted the benefits of 2D simulations for reducing computational costs while retaining critical detonation characteristics.

4. Performance Metrics

The performance of each RDE was evaluated using key metrics such as detonation wave speed, thrust, specific impulse, and pressure gain. It is important to note that these performance metrics cannot be directly compared against one another, as they are heavily influenced by the experimental setup, geometric configuration, fuel and oxidizer selection, and test conditions. Some values were obtained through direct physical testing, while others were derived from computational simulations, each with its own inherent assumptions and limitations. Understanding the context of each study is essential for accurately interpreting these performance results.

5. Key Findings and Notable Observations

The comparative analysis reveals several key findings:

- Annular geometries remain the most widely studied, but alternative designs like disk and cone configurations demonstrated unique benefits.
- Hydrogen-air is the most frequently used propellant, but methane-oxygen has been explored for its stability.
- Numerical simulations provide valuable insights at reduced costs, especially when employing 2D configurations.

This comparative analysis provides a clear understanding of the advancements and challenges in RDE research, guiding future investigations toward optimizing geometry, fuel selection, and testing methodologies.

1.4 Project Objective

The main objective of this project is to conduct a comprehensive literature review of worldwide RDE combustion chamber geometries to determine the best method to optimize performance metrics. The study will examine various geometric configurations, including annular, hollow, cone, and disk-shaped designs, along with their specific dimensions. This review aims to enhance understanding of geometric setups, as well as fuel and oxidizer selection, providing a foundation for improved RDE performance.

Initially, the intention was to create 3D CAD models for each configuration and simulate them using ANSYS Fluent. However, due to computational resource limitations, the scope has been adjusted to focus on a 2D unrolled geometry. This 2D approach offers a simplified yet accurate representation of the RDE's internal flow dynamics, making it feasible for detailed computational analysis while maintaining the ability to capture essential detonation behavior.

1.5 Methodology

The methodology for this project will begin with a comprehensive literature review focused specifically on 2D RDE simulations. The review will gather and analyze data from the most relevant studies worldwide that have utilized 2D modeling approaches for RDEs. This will include examining different geometric configurations, such as unrolled annular, rectangular, and linear channel designs, and understanding how these simplified 2D models are used to accurately replicate the complex flow dynamics of RDEs. The primary objective of the literature review is to identify the best methods for setting up the 2D RDE simulations, including chamber size, inlet configuration, boundary conditions, and numerical models. Key parameters such as channel length, width, ignition methods, and the type of fuel-oxidizer mixtures will be investigated. The review will also compare the performance metrics reported in these studies, such as detonation wave speed and possibly thrust.

Following the literature review, a comparative analysis will be conducted to determine which 2D geometric configuration offers the most optimized performance characteristics. This analysis will serve as the foundation for the 2D computational model to be developed in ANSYS Fluent. A 2D unrolled geometry will be selected for further analysis, where the detonation wave propagation, flow dynamics, and thrust generation will be looked into. The ultimate goal is to establish a clear understanding of how to properly set up and optimize a 2D RDE simulation, ensuring accurate and efficient computational analysis. This approach helps overcome the computational challenges of 3D modeling while providing valuable insights into the performance of RDEs.

Chapter 2: Background, Theory, & Governing Equations

This chapter provides a comprehensive background of the underlying thermodynamic principles, detonation wave theory, and governing equations relevant to rotating detonation engines. Topics that will be discussed include pressure gain combustion within the Humphrey cycle, Rankine–Hugoniot relations, the development of the Chapman-Jouguet and ZND detonation models, and the mathematical framework for modeling detonation behavior. As mentioned in chapter 1, this chapter will also further investigate the foundational experiments conducted in the 1950s, specifically by Bogdan Voitsekhovsky. These early experiments laid the groundwork for the development of rotating detonation engines as well as provided the initial framework for both experimental setups and numerical modeling strategies that are still built upon today, which is why it's critical to understand. Chapter 3 will numerically implement the theories discussed and provide a demonstration with the utilization of NASA CEARUN Code and Ansys Fluent.

2.1 Historical Background & Foundational Experiments

The utilization of the detonation process for the means of generating power or propulsion was first discovered in 1881 by a group of French scientists named Berthelot, Vieille, Mallard, and Le Chatelier [30]. They were the first ones to observe gaseous detonation waves in shock tubes and from their findings, they were able to determine a new combustion process method besides deflagration. Differences between the two will be further discussed in the upcoming sections as well as specific distinctions and their importance.

The next critical discovery happened in the early 1900's, when David Chapman and Émile Jouguet were able to provide the mathematical predictions of detonation wave propagation, which are known to be the Chapman-Jouguet conditions. Then in the 1940's, John von Neumann and Werner Döring were able to provide the structure of the detonation wave, which was later reinforced by Yakov B. Zel'dovich and Aleksandr Solomonovich Kompaneets in the 1960s, which is known as the ZND model [30]. These specific discoveries are considered the fundamental framework required for understanding and experimentation with detonation wave propagation for the generation of propulsion and will be further discussed in the next couple of sections more in depth.

During the 1950's, the research and experimentation regarding detonation waves became more and more popular. As discussed in the previous chapter, Professor James Arthur Nicholls from the University of Michigan successfully built and tested one of the first ever pulse detonation engines. However, due to the lack of technology during this time, it was extremely difficult to make further advancements.

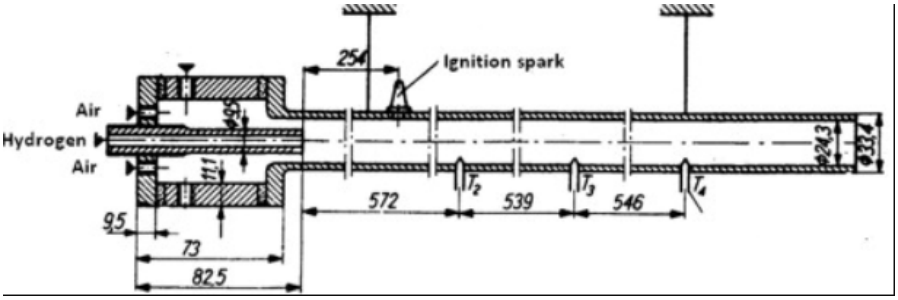

Figure 2.1 - PDE testing set up [31]

Another physicist, Bogdan Voitsekhovsky, was able to successfully conduct experimentation on obtaining the structure of spinning detonation waves, particularly their three-dimensional aspects in confined geometries. His study was able to provide a detailed framework for the numerical development of the mathematical model required for sustaining detonation waves, which will now be further analyzed in order to gain a deeper and more in depth understanding.

Voitsekhovsky studied many different elements and components of what is known as current rotating detonation engines. As stated previously, one of his most critical investigations consisted of the observation of spinning detonation waves in an annular and cylindrical combustion chamber. He found that the detonation wave would rotate "azimuthally along the inner wall of a chamber, rather than traveling linearly down a tube" [5]. This was the first ever documentation of a sustained rotating detonation wave. His experimental set up is still being used today as the basis for the majority of the RDE research. The figure below provides an example of description of the spinning detonation, provided by the The History of the Study of Detonation article.

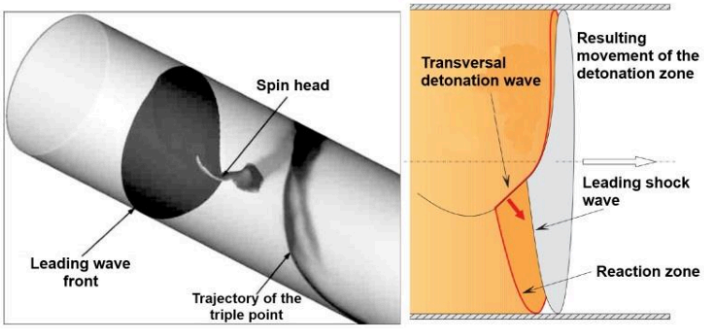

Figure 2.2 - Spin detonation structure in a channel [32].

Additionally, his work also highlights numerous investigations done prior to his, as well as the mathematical concepts used, such as the CJ theory, ZND model, and the theoretical background on the thermodynamic principles, all of which is important for the overall understanding of how RDE's work. This can be seen in his studies consisting of the research into the motion and structure of detonation waves, multiple-front detonations, spin detonations, and even stationary detonations [5]. For the stationary detonation experiment, the experimental setup can be seen

down below. This study would be able to provide data on the structure of a detonation wave, distribution of density, pressure, temperature, and the kinetics of chemical reactions [5]. A stoichiometric mixture of oxyacetylene was used.

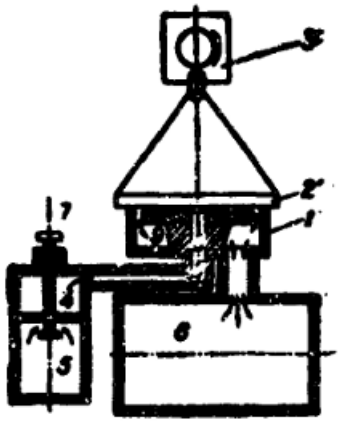

Figure 2.3 - Experimental set up for annular gap testing [5].

Another one of his studies consisted of the investigation of the confinement and chamber geometry and its effects on the detonation wave behavior. The three geometries he studied were an annular, cylindrical, and rectangular combustion chamber. He specifically investigated the effects of the boundary conditions, channel width, and the curvature affected the wave formation, stability, and propagation. He was the first one to propose that by burning the mixture in the detonation mode would help achieve more stable rotating waves, very specifically, transverse waves of a spinning configuration [5]. His work is still being studied today, as it provides crucial information on the optimal testing, setup, and experimentation of continuous rotating detonation waves.

2.2 Thermodynamic Principles

When specifically looking at the thermodynamic cycle, rotating detonation engines fall under the Humphrey's cycle as its the theoretical basis for utilizing pressure gain combustion, which is the process that allows for the pressure of the working fluid to increase during combustion and allows for the rapid energy release of detonation or near-detonation processes. This is what generates shock waves that compress the fluid in front of the reaction zone. The main difference between the Humphrey's cycle and other cycles such as the Braytons cycle, lies in its heat addition process. For the Humphrey's cycle, the volume is held constant, but heat is being added, which in turn intensifies the pressure during combustion. For the Braytons cycle, the pressure remains constant while heat is being added and the volume increases [1].

From the figure seen below, it is clear that the Humphrey cycle is more efficient than the Brayton's cycle. The main theoretical benefits that can be observed with pressure gain

combustion, is its ability to reduce entropy generation, increase thermodynamic efficiency, reduce specific fuel consumption to fuel burned, thrust-to-weight ratios, and can even reduce carbon dioxide emissions [28].

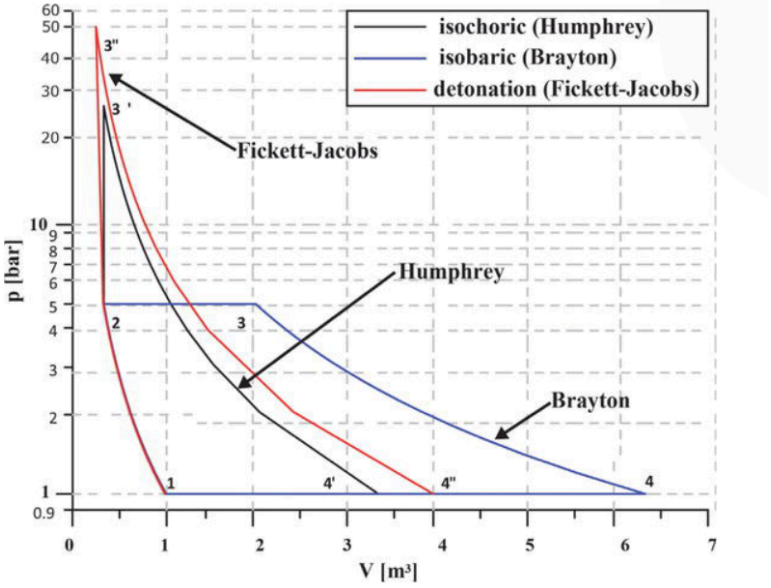

Figure 2.4 - Thermodynamic cycles of Humphrey's, Braytons, and Fickett-Jacob [33].

2.3 Detonation Wave Models

2.3.1 Deflagration vs Detonation

The key distinctions between traditional day rocket engines and rotating detonation engines lie in the combustion type they utilize. Conventional engines utilize deflagration waves as a means of producing thrust, while rotating detonation engines harness the power of detonation waves. It is important to define the similarities and differences between detonation and deflagration in order to fully understand the capabilities and limitations of both combustion types.

Deflagration waves have been used as the main basis of combustion propulsion for rocket engines ever since the 1960's. It can be described as a subsonic combustion process, which is below Mach 1, that utilizes heat and mass transfer of the unburned mixture for the propagation of the combustion waves through the combustion chamber, which typically leads to the decrease in the pressure and density [1]. In contrast, detonation works by the leading supersonic combustion driven shock wave, which is above Mach 1, that compresses the mixture, where it is then followed by the reaction zone that triggers the chemical reaction and releases energy due to the increase in temperature and pressure, that leads to the propagating detonation waves.

The primary advantages of detonation-based combustion over traditional deflagration include a significant increase in thrust performance and thermal efficiency, estimated to be approximately 25 percent, as well as reduced fuel consumption and enhanced specific impulse. Detonation enables pressure gain combustion, which allows for the high increase in pressure assisting the overall propagation of powerful detonation waves. This also allows for an extremely compact design that eliminates the need for any moving components, such as a large compressor typically found in traditional rocket engines. Furthermore, this allows for structural simplicity and ease of manufacturing.

Deflagration is typical in conventional propulsion systems, such as gas turbines, ramjets, and liquid-fueled rockets, whereas detonation is observed in high explosives and is now being investigated for advanced propulsion concepts like rotating detonation engines, due to its groundbreaking technological advancements. A deeper understanding of detonation physics can be obtained by analyzing the governing models that describe its propagation behavior, beginning with the Rankine–Hugoniot relations, which apply the fundamental conservation laws across the detonation front. These relations form the basis for more detailed models, namely the Chapman–Jouguet (CJ) theory and the Zel'dovich–von Neumann–Döring (ZND) model, both of which are presented in the following sections.

2.3.2 Rankine–Hugoniot Relations

The Rankine–Hugoniot relations describe the conservation of mass, momentum, and energy across a discontinuity such as a shock wave or detonation front. They are derived from the integral form of the conservation laws and apply to one-dimensional, steady flows in a control volume that spans a thin wave front. This means that it can be applied to multiple models that include any discontinuity where a sudden change in flow properties occurs such as shock wave, deflagration, and detonation. Specifically for detonation theory, they are used to relate the pre-detonation (reactants) and post-detonation (products) states of the gas [29]. The main assumptions to be made include an inviscid and adiabatic flow, instantaneous transition across the wave front, and the thermodynamic equilibrium on both sides of the wave, which is required for the Chapman-Jouguet theory. The simplified schematic of the one dimensional combustion wave can be seen in Figure 2.5, which helps provide a visual representation of how and where the conservation equations are used.

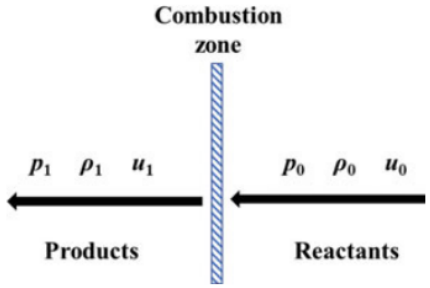

Figure 2.5 - Schematic representation of 1D combustion wave [29]

With the assumptions made, the conservation equations can now be investigated. Subscripts 1 denotes the pre-wave states, while subscript 2 denotes the post-wave states. The conservation equations consist of the mass, momentum, and energy. The mass equations relate to the mass flow rate being conserved across the shock wave, the momentum change is in relation to the pressure jump, and the energy equation shows the total energy remaining constant across the front. However, the heat release amount per unit mass is the unknown variable, which is accounted for through the temperature and product fractions when calculating the post wave equilibrium states [29].

$$\rho_0 u_0 = \rho_1 u_1 = \dot{m} \tag{2.1}$$

$$\rho_0 u^2_0 + p_0 = \rho_1 u^2_1 + p_1 \tag{2.2}$$

$$h_0(T_0) + \frac{u^2_0}{2} + q = h_1(T_1) + \frac{u^2_1}{2} \tag{2.3}$$

With these core conservation equations, it is now possible to solve for the pre and post shock wave conditions. Additionally, it also provides the ability to derive the Rayleigh line and the Hugoniot curve. The Rayleigh line is derived by the conservation of mass and momentum equations as it expresses the relationship between the pressure and specific volume, where the specific volume is the inverse of the density.

$$p_1 = (p_0 + \dot{m}^2 v_0) - \dot{m}^2 v_1 \tag{2.4}$$

The Hugoniot curve is specifically derived from the conservation of mass and energy equations as this presents all thermodynamically possible post-detonation states. This equation will vary as it depends on the initial conditions and the energy content of the mixture, specifically the heat release.

$$h_1 - (h_0 + q) = \frac{1}{2}(p_1 - p_0)(v_0 + v_1) \tag{2.5}$$

The relationship between the Rayleigh line and the Hugoniot curve broken down into 5 zones depending on the strength of the detonation can be seen down below. For instance, zone 1 is considered a strong detonation zone, zone 3 is the weak deflagration zone, and zone 5 is the no solution zone. The trend can be very clearly seen, including the two main intersection points between the Rayleigh line and the Hugoniot curve. The upper point is where the compression zone is, and this is where the Rayleigh line is tangent to the Hugoniot curve. This point specifically provides the solution to the Chapman-Jouguet detonation. This instance also holds true for the lower point, however it would coincide with the Chapman-Jouguet deflagration.

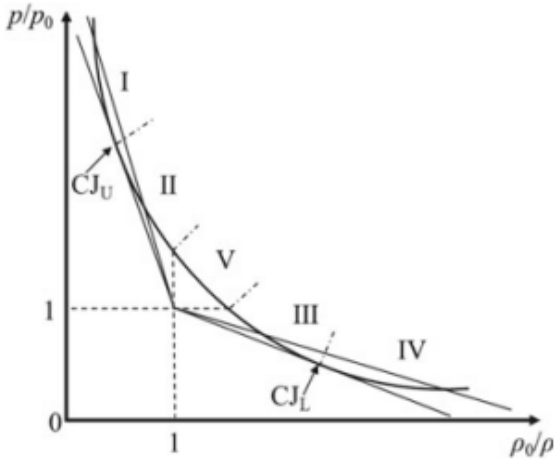

Figure 2.6 - Rayleigh line and Hugoniot curve [29]

The upper CJ point is where the minimum detonation velocity can be obtained, as the tangent Rayleigh line signifies sonic flow conditions behind the detonation wave. The simplified equation for the CJ detonation speed can be seen in equation 2.5. This equation is an estimate as it is assumed that the heat release amount is large. More about the Chapman-Jouguet theory will be discussed in the next section, as this theory is critical for understanding and obtaining post detonation wave parameters.

$$U_{CJ} = \sqrt{2(\gamma^2_1 - 1)q} \tag{2.5}$$

2.3.3 CJ Theory

The Chapman Jouguet theory specifically details the model of a steady state detonation wave, with a particular focus on the thermodynamic conditions at the end of the reaction zone. It is able to obtain the minimum velocity required to sustain a propagating detonation wave, the specific point where the combustion products are moving at sonic speed behind the detonation front, as well as allowing for the calculation of key detonation properties such as the post-detonation pressure, temperature, and density for a given fuel–oxidizer mixture [29]. This sonic condition is critical because it prevents any disturbances or feedback from influencing the detonation front, thus making the wave self-sustaining. The two primary parameters influencing the CJ speed are the heat release per unit mass and the ratio of specific heats of the mixture. If there is a decrease in specific heat ratio, the detonation velocity also decreases. Below is the list of equations behind the CJ detonation, consisting of density, pressure, velocity, and mach number [34].

$$\frac{\rho_{CJ}}{\rho_0} = \frac{\gamma+1}{\gamma} \tag{2.6}$$

$$\frac{p_{CJ}}{p_0} = \frac{\gamma M_{CJ}^{\ 2}}{\gamma+1} \tag{2.7}$$

$$\frac{u_{CJ}}{V_{CJ}} = \frac{\gamma}{\gamma+1} \tag{2.8}$$

$$M_{CJ} = \frac{V_{CJ}}{a_0} \tag{2.9}$$

A key limitation of the CJ model is its simplification of the internal structure of the wave—it does not account for the finite-length reaction zone or the induction time before ignition. This makes it insufficient for modeling instabilities, cellular detonation, or transient behavior, particularly in systems like rotating detonation engines. To address this, a more detailed approach is provided by the ZND model, which incorporates the internal dynamics of the detonation front and reaction kinetics.

2.3.4 ZND Model

The ZND model is able to provide a more detailed representation of detonation physics by resolving the internal structure of the detonation wave. The ZND model incorporates finite-rate chemical kinetics, allowing for a time- and space-resolved description of the wave, whereas the CJ model only treated the detonation front as an infinitesimally thin discontinuity. The ZND detonation model is assumed to be a perfect gas with a fixed specific heat capacity ratio, and the reaction following the Arrhenius law.

This one-dimensional, steady-flow, model, the detonation wave is broken down into 4 specific regions which will provide a more in depth explanation of the entire process of the detonation wave. These regions consist of a leading shockwave, induction zone, reaction zone, and expansion zone [29]. The leading shock wave is where there is a strong, nearly instantaneous compression which increases the temperature and pressure of the unburned mixture. The induction zone is considered the delay region as this is where the chemical reactions are initiated but not yet substantial, however the energy is being absorbed as the bonds are beginning to break. The reaction region is where the exothermic reaction occurs rapidly, where heat is released and in turn accelerates the flow. The CJ plane is the specific point at which the flow becomes sonic relative to the wave front. Finally, the expansion zone is where the products are expanded out and cooled as they move downstream.

In summary, as the shock compresses the reactants, it causes a release of chemical energy, an acceleration in products, the generation of the CJ plane, and the product expansion as it is expelled. These regions can be visualized on the ZND structure diagram below, where pressure, temperature, and density evolve continuously behind the shock. The ZND model demonstrates how the energy from the initial shock is transferred into thermal energy, which then sustains the wave through chemical heat release. This mechanism is critical for understanding detonation stability, cellular structures, and wave curvature effects, all of which are highly relevant for rotating detonation engines.

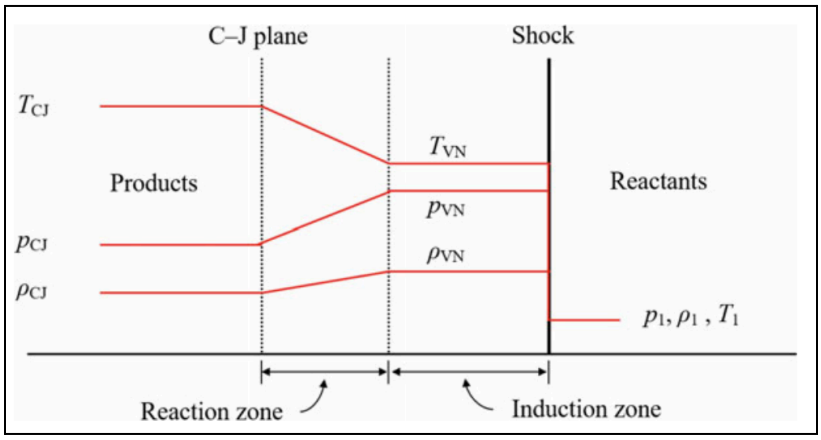

Figure 2.7 - Schematic of ZND model [29].

While the ZND model is based on the same conservation principles of mass, momentum, and energy as described in the previous section, it reformulates these equations into a system of ordinary differential equations, specifically when given the chemical reaction rate, that describe how thermodynamic and chemical properties evolve spatially behind the shock front. Assuming the simplest mode of the one-step heat release model, the chemical reaction rate can be written in

the Arrhenius form, where two constants represent the pre-exponential factor, k, and the activation energy, Ea.

$$\frac{d\lambda}{dt} = k(1 - \lambda)e^{\frac{-E_a}{RT}} \tag{2.10}$$

This equation provides the necessary calculations for a steady ZND structure. In summary, by assuming a value to gamma and the heat release, the CJ velocity can be calculated. Then the post shock states can be determined such as the temperature and pressure, when analyzing the Rankine-Hugoniot relations [29]. The ZND model provides a visualization of the change in temperature and pressure leading up to the CJ conditions. This is where there should be an observation of a rapid decrease in pressure while the temperature quickly increases. However, due to current technological advancements, many softwares such as NASA CEA RUN, have been created to help with calculation of such complex problems, CJ Detonation parameters being one of them. A more in depth explanation and a step by step guide on the setup will be provided in the next chapter.

Chapter 3: Fuel & Oxidizer

3.1 Background Research

Selecting the appropriate fuel and oxidizer is critical as it directly impacts the overall performance of the RDE. The article that analyzed the development of trends in RDE's done worldwide, highlights the various fuel and oxidizer combinations used by different institutions [4]. Among these, hydrogen and air are commonly chosen due to their popularity and proven effectiveness. In this portion of the project, an investigation will be conducted using Python and Cantera to calculate the thermodynamic equilibrium properties of the most widely used fuel-oxidizer mixtures in RDEs. This analysis will help identify the strengths and weaknesses of each mixture, ultimately guiding the selection of the most optimal mixture for this project. The specific thermodynamic properties to be extracted include temperature, pressure, density, enthalpy, entropy, Gibbs free energy, and heat capacity.

3.2 Thermodynamic Analysis of Multiple Mixtures

The fuels investigated in this analysis include hydrogen (H2), methane (CH4), ethane (C2H6), ethylene (C2H4), and propane (C3H8), each paired with oxygen (O2) and air as their oxidizer. The results provide important insights into the performance of each fuel-oxidizer combination in terms of temperature, Gibbs free energy, and enthalpy, which are crucial for optimizing a RDE. The table below provides all the results obtained from the thermodynamic analysis done in Cantera and Python. Based on the analysis, hydrogen with air produces a temperature of 1938.21 K, a Gibbs free energy of -2.7E+07 J/mol, and an enthalpy of 3511.75 J/mol, making it one of the top contenders in terms of both energy release and combustion efficiency. This choice aligns with the majority of real-world RDE studies, which commonly use hydrogen and air due to their practical and widespread application in the aerospace industry.

While hydrogen with air is a highly promising mixture, its slightly lower temperature and energy release compared to other combinations like hydrogen with oxygen or ethylene with oxygen, make it a slightly less optimal choice for pushing performance to its highest limits. Hydrogen and oxygen produced the highest temperature of 2911. 27 K, enthalpy of 3166.91 J/mol, and a Gibbs free energy of -4E+07 J/mol. Ethylene and oxygen however, provided the best balance of high temperature at 2330.22 K, Gibbs free energy of -3.6E+07 J/mol and an enthalpy of 876466.32 J/mol. This mixture stands out as the most efficient and effective combination for achieving high energy output and optimal combustion.

Nevertheless, hydrogen with air remains an ideal selection for this project due to its reliability, proven effectiveness, and the ability to easily compare results with existing research. The thermodynamic properties for this mixture, including its temperature, Gibbs free energy, and

enthalpy, demonstrate that it provides a solid foundation for achieving efficient detonation in an RDE. By choosing hydrogen with air for the study, this project ensures that it is aligned with real-world practices while still providing valuable insights into the performance of different fuel-oxidizer combinations in RDE systems.

$$2H_2 + (O_2 + 3.76N_2) \rightarrow 2H_2O + 3.76N_2 \quad (3.1)$$

Table 3.1 - Fuel & oxidizer thermodynamics properties [35].

Fuel	Oxidizer	Temperature (K)	Pressure (Pa)	Density (kg/m^3)	Molar Enthalpy (J/mol)	Molar Entropy (J/mol/K)	Molar Gibbs Free Energy (J/mol)	Molar Heat Capacity (J/mol/K)
H2	O2	2911.27	101325	0.09	3166.91	13596.62	-4E+07	2244.49
H2	air	1938.21	101325	0.11	3511.75	14042.51	-2.7E+07	2255.6
CH4	O2	2610.67	101325	0.07	-1550324	16272.73	-4.4E+07	2688.9
CH4	air	833	101325	0.28	-1658998	11929.25	-1.2E+07	2229.88
C2H6	O2	1236.74	101325	0.12	-1348511	16519.64	-2.2E+07	2612.1
C2H6	air	853.87	101325	0.31	-1420533	11166.68	-1.1E+07	2381.81
C3H8	O2	1281.84	101325	0.14	-1362278	15156.93	-2.1E+07	2835.58
C3H8	air	589.65	101325	0.51	-1421045	9840.4	-7223482	2085.4
C2H4	O2	2330.22	101325	0.08	876466.3	15694.76	-3.6E+07	2399.93
C2H4	air	1059.24	101325	0.28	924955	10762.77	-1E+07	2254.3

3.3 NASA CEARUN Software

The NASA CEARUN software was used to calculate the detonation parameters for the given fuel and oxidizer ratio. This software allows for the calculation of any chemical equilibrium for specific problem types, more of which can be found on the introduction webpage, which also includes a more detailed explanation [36]. In this case, the Chapman-Jouguet Detonation problem type was selected. Then, for the initial conditions, temperature was set at 300 K, and the pressure was set to 1 Pa. Fuel and oxidizer were chosen to be hydrogen and air, and the

proportion of this mixture was set to the equivalence ratio of 1, to simulate a stoichiometric ratio. The initial parameters chosens can be seen in the figure below. From here, the results were calculated and outputted, which can be seen in the corresponding tables below.

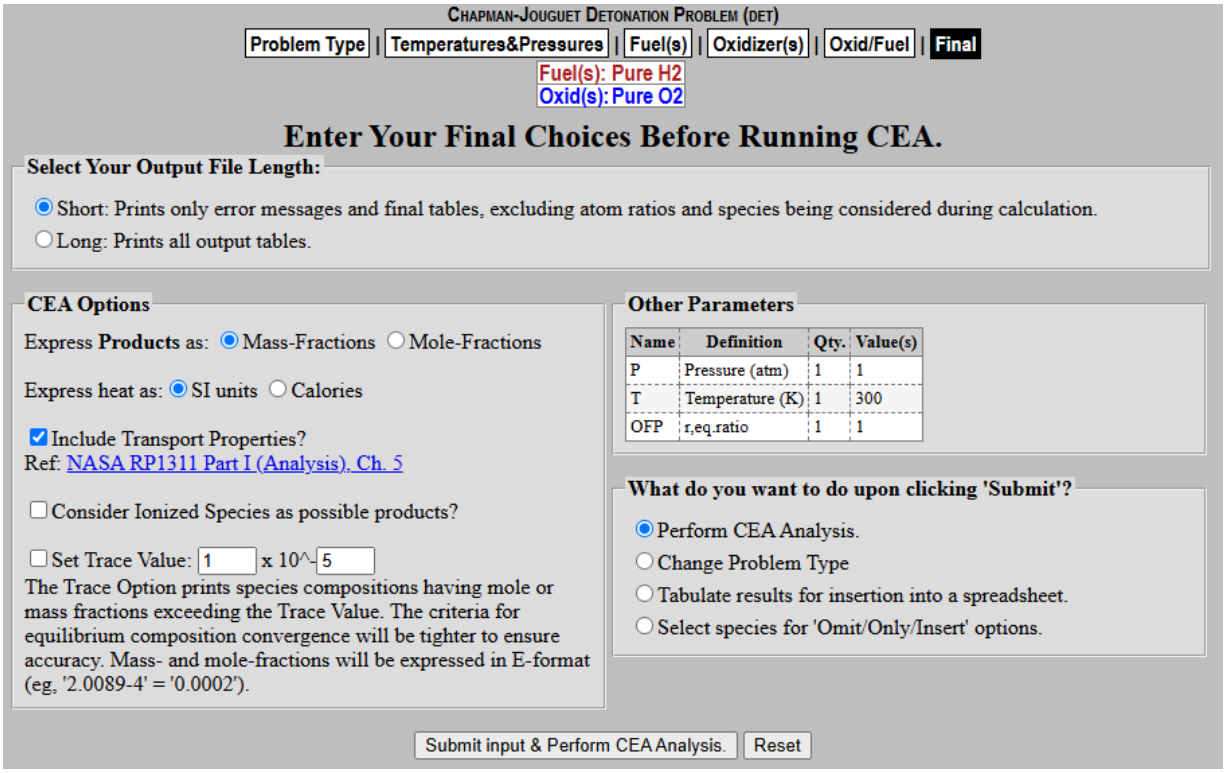

Figure 3.1 - Input of results before CEA analysis [37].

Table 3.2 - Initial conditions of unburned gas [37].

Property	Value
Pressure (P1)	1.0132 bar
Temperature (T1)	300 K
Enthalpy (H1)	-1.65 KJ/kg
Molar Mass (M1)	21.008 n^-1
Gamma (Ɣ1)	1.4014
Speed of Sound	407.9 m/s

Table 3.3 - Detonation parameters [37].

Property	**Value**
P/P1	15.491
T/T1	9.813
M/M1	1.1427
RHO/RHO1	1.8039
Detonation Mach Number	4.8169
Detonation Velocity	1964.9

Table 3.4 - Initial conditions of burned gas [37]

Property	**Value**
Pressure (P2)	15.696 bar
Temperature (T2)	2943.85 K
Density (ρ)	1.5394 kg/m^3
Enthalpy (H)	1335.47 KJ/kg
Internal Energy (U)	315.89 kJ/kg
Gibbs Free Energy (G)	-29842.8 kJ/kg
Entropy (S)	10.5910 kJ/kg*K
Molar Mass (M)	24.007 g/mol
Specific Heat Capacity (Cp)	3.3589 kJ/kg*K
Gamma (ϒ)	1.1636
Speed of Sound	1089.2 m/s

Table 3.5 - Mass fractions of burned gas [37].

Species	Mass Fraction
Ar	0.01255
CO	0.00013
CO2	0.00026
H	0.00025
HO2	0.00002
H2	0.00263
H2O	0.22026
NO	0.00944
NO2	0.00001
N2	0.72937
O	0.00136
OH	0.01356
O2	0.01014

Chapter 4: Research and Implementation of 2D model

The original objective for this project was to perform three-dimensional simulations of the multiple RDE combustion chamber geometries, including an annular, hollow, disk, and cone-shaped configurations. However, due to significant constraints in computational resources and high simulation time required for 3D modeling, the scope of the project was adjusted to focus on two-dimensional simulations.

In response to this shift, a thorough investigation into two-dimensional modeling was conducted and will be further discussed in the next section. However, this literature review was able to confirm that a substantial number of studies were able to demonstrate and confirm that 2D simulations can effectively capture many of the critical physical phenomena associated with detonation wave propagation, such as wave structure, speed, and post detonation parameters. The main similarity seen in these studies is the implementation of the 2D "unrolled" or "unwrapped" annular geometry, which have been successfully used to replicate 3D detonation behavior with reasonable accuracy and greatly reduced computational cost. The model below provides a visual where the curvature of the annulus is transformed into a planar domain as well as the boundary conditions and dimensions.

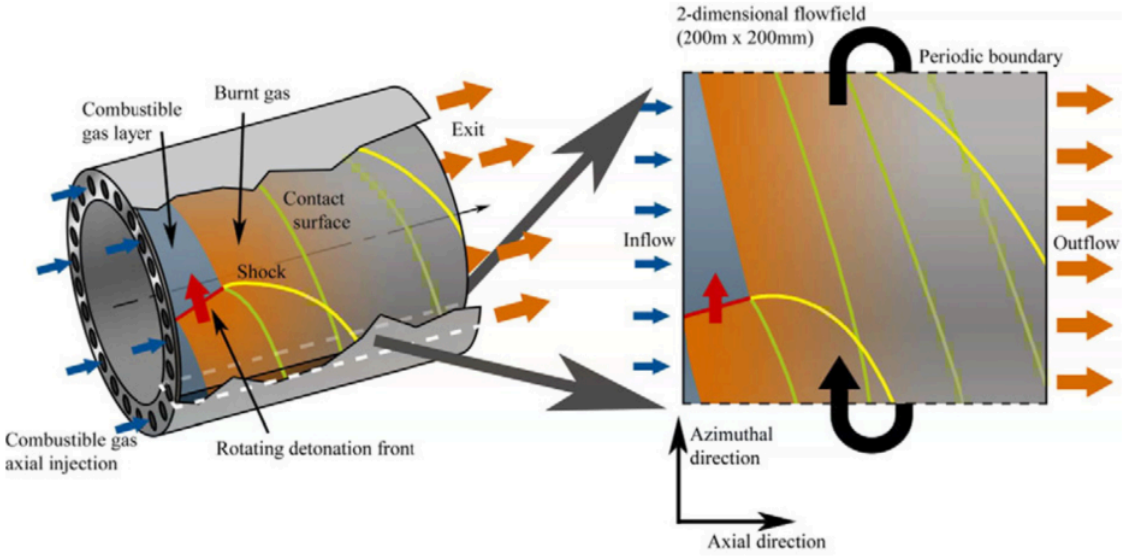

Figure 4.1 - Unrolled annular geometry [1]

4.1 Literature review of 2 Dimensional RDE simulations

For this literature review, an extensive investigation will be conducted into multiple 2 dimensional studies to evaluate how their modeling approaches, boundary conditions, and numerical frameworks can inform and enhance the current project's simulation setup. Key focus areas include the computational software utilized, the selected fuel and oxidizer combinations, initial and boundary conditions, governing physical models and equations, and the numerical methods implemented for detonation modeling. Additionally, the results obtained in each study will be carefully reviewed. A comparative analysis will be done on these parameters to determine which configurations, assumptions, and modeling strategies are most suitable for integration into this project's current simulation framework.

4.1.1 Numerical Simulation of 2D Premixed Combustion Article

This study focuses on numerically analyzing the flow dynamics within a 2 dimensional premixed combustion RDE model. Due to the limited number of detailed investigations in this area, the objective of the simulation was to characterize key flow behaviors such as detonation wave propagation, shock interactions, pressure and temperature distributions, and detonation front dynamics.

The simulation was performed using ANSYS Fluent, modeling a hydrogen–air mixture with a 10-species, 21-reaction finite-rate chemistry mechanism [38]. A simplified 2D geometry, with a dimensional domain of 70 mm length and 20 mm height, was used to reduce computational cost while still capturing the critical detonation physics. The inlet condition was assigned a mass flow inlet with a total mass flux of 357 kg/m^3, equivalence ratio of 1, and an inlet temperature of 300 K [38]. This is where the premixed hydrogen-air mixture will be injected. The outlet boundary was assigned to be a pressure outlet with initial conditions of a pressure of 1 bar and a temperature of 300 K [38]. These outlet conditions were chosen to prevent undesired wave reflections and resonance effects within the chamber.

Initially, the left and right boundaries were set as non-slip adiabatic walls, effectively preventing the detonation wave from propagating laterally. However, once a stable detonation wave began forming and traversing the width of the domain, the simulation was paused. The boundary conditions were then switched to translational periodic boundaries, which helped enable a continuous detonation wave propagation through the fresh mixture and prevented wave collision due to reflected shocks caused by the initial pressure imbalance [38].

To further reduce computational complexity, a surrogate air mixture was utilized, which consisted of 78.084% nitrogen and 20.9476% oxygen. This maintains stoichiometric balance while minimizing simulation overhead. The table below provides the species mass fractions for this mixture.

Table 4.1 - Mass fraction for stoichiometric mixture of H2/Air [38].

Species	Reactants(%)	Products(%)
H_2	0.0287	0.2565
O_2	0.2278	0
N_2	0.7435	0.7435

For their ignition strategy, a direct ignition approach was employed by initializing a localized region of 0.5 mm × 5.0 mm within the domain at a temperature of 3500 K and pressure of 30 bar [38]. This strategy was successful in initiating the detonation wave. The figure below provides a visual of the location of the ignition region and the parameters.

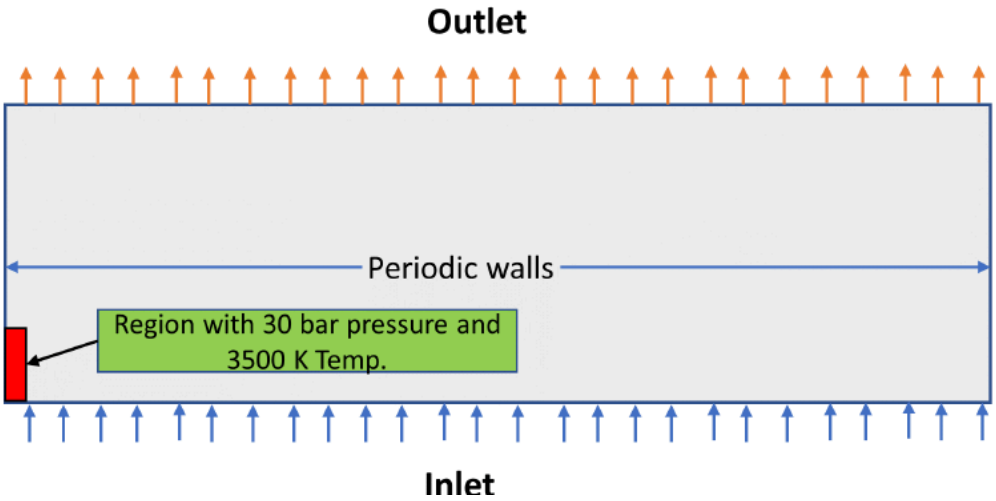

Figure 4.2 - Layout and direct ignition in RDE chamber [38].

For the numerical solvers, they utilized the Reynolds-Averaged Navier–Stokes (RANS) equations to model turbulent flow behavior, a k–ω SST two-equation turbulence model, and a finite-rate chemistry (FRC) model to compute local reaction rates based on actual chemical kinetics rather than assuming equilibrium [38]. In addition, species transport equations were solved to account for diffusion and reactions, and the Arrhenius rate law is used to assist with the incorporation of the detailed chemical kinetics [38].

To ensure numerical stability and maintain accuracy, a 2D transient approach was taken, along with spatial discretization set to a second order upwind, and temporal discretization set to first-order implicit [38]. The Courant–Friedrichs–Lewy (CFL) number was maintained between 0.6 and 0.8, and a time step size of 5×10^{-8} seconds was selected. This allows for high temporal resolution and ensures the reliable convergence of transient detonation phenomena.

Additionally, they also performed a mesh sensitivity study with a uniform mesh size of 0.1 mm, 140,000 quadrilateral elements, was selected as the optimal resolution. This mesh configuration

successfully captured the shock structure and peak temperatures, with a recorded maximum of 3590 K and from their simulation results, a detonation wave speed of 1880 m/s was achieved with a percent error of approximately 4 percent when compared to the theoretical CJ velocity [38].

4.1.2 Modeling 2D Linear Detonation Engines Article

This study focuses on simulating a simplified 2D RDE geometry operating with a gaseous kerosene-air mixture, utilizing the ANSYS Fluent software. The primary objective is to observe a steady wave propagation and gain experimental insight on the wave structure, basic parameters, and then have them compared to data in the literature [39]. Notably, processes such as fuel injection, evaporation, and upstream mixing are omitted, with the assumption that they occur prior to the combustion zone as this allows for the assumption that this all takes place upstream of the combustion zone [39].

The dimensions of the combustion chamber are modeled to be 452 mm wide and 100 mm long. A uniform quadrilateral mesh is employed, consisting of 904 × 200 cells in the horizontal and vertical directions, respectively. This results in a cell size of 0.5 mm × 0.5 mm, suitable for capturing critical detonation dynamics within computational limits. The inviscid model is selected in ANSYS Fluent to simplify the analysis, assuming that viscous and diffusive effects are negligible due to the coarse mesh and absence of solid boundaries [39]. This assumption is widely adopted for similar detonation modeling applications. The chemical reaction is modeled as a single-step global mechanism describing kerosene and oxygen combustion. The reaction becomes active above 350 K to prevent numerically-driven autoignition, meanwhile the Arrhenius rate expression is used where the pre-exponential factor A is 2.587·10^9, and the activation energy EA is 1.005·10^8 J/kmol [39]. Nitrogen is treated as an inert species and does not participate in the reaction.

The boundary conditions for the inlet consist of fresh stoichiometric kerosene-air mixture entering at a pressure of 1 bar and temperature of 300 K, with a vertical velocity of -150 m/s, representing perpendicular inflow, and a mass flow rate is set to 82.8 kg/s [39]. The outlet boundary however, is defined as the pressure outlet, but more specifically, the reflecting pressure outlet. This is to allow for the replication of post detonation conditions for the possibility of backflow occurring. This boundary is set to a temperature of 3000 K, and the species composition resembles the products of the chemical reaction [39].

For the domain composition, the top 5% near the inlet, is filled with the fresh incoming reactant mixture, and the other 95% of the domain is initialized with the products of the ideal kerosene-air combustion. For the ignition, the detonation is triggered by initializing a small patch within the post-combustion zone. This region is defined by a temperature of 1500 K, pressure of 150 bar, and a velocity in the x direction of 1500 m/s [39].

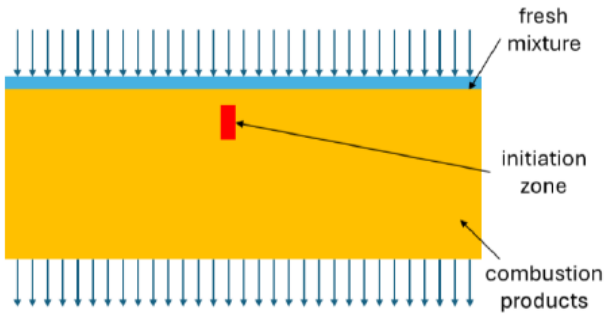

Figure 4.3 - Initial conditions and domain composition [39].

The simulation employs a density-based solver with an implicit formulation and Roe-FDS flux scheme, where the spatial discretization of gradients is handled by using a last-squares cell-based, 2nd order upwind method is used to discretize using the flow equations, and temporal discretization is carried out using an implicit second-order scheme [39]. The chemical kinetics are integrated using a stiff solver to handle the chemical stiffness inherent in detonation modeling, while the courant number is set to 2.5, which yields a time step of 3x10^-7 seconds, with up to 30 sub-iterations per time step to ensure convergence [39].

This simulation setup successfully demonstrates the ability to capture detonation propagation in a simplified 2D linear engine model. They were able to obtain a wave speed of 2176 m/s, whereas the calculated CJ velocity was equal to 1789 m/s [39]. The results from the simulation were 21% higher than the calculated, which was due to the oversimplified combustion model, as the one used for the CJ velocity calculation provides the detailed list of many species. This is a very important key detail to note, as there may be a trend in the discrepancy between the experimental data and theoretical data, specifically for the detonation wave velocity, not just with this article, but others.

4.1.3 Simulation of Continuous Spin Detonation Article

This study investigated the phenomenon of continuous spin detonation (CSD) in a two-dimensional annular geometry of the combustion chamber, with a hydrogen-oxygen mixture using ANSYS Fluent. The primary objective was to numerically simulate the propagation of CSD waves under various conditions and compare the results with experimental data.

The core governing equations were the unsteady Reynolds-averaged Navier–Stokes (URANS) equations, with turbulence effects modeled using the k-ε model, along with the FRC model that accounted for 21 reactions in a 10-species hydrogen-oxygen mixture [40]. The simulations used the ISAT (In-Situ Adaptive Tabulation) algorithm for chemical kinetics, which enhanced convergence even with stiff reaction mechanisms. A pressure-based coupled solver was used, with second-order central difference for momentum equations, second-order upwind for energy

equations, and first-order implicit time discretization, along with a courant number between 0.6 to 0.8 to allow for a stable solution, and a time step size of 5 x 10^-8 s [40].

The computational domain measured 70 mm in length and 30 mm in height. The mesh was refined using a second-order gradient adaptation with the initial grid size set at 0.2 mm, making sure the total number of cells was not over 512,000 [40]. Detonation was initiated using local semi-circular high-energy regions with a radius of 1 mm, a pressure of 30 atm, and a temperature of 3000 K [40]. The initial mixture in the domain was set at 300 K and 1 atm for the nitrogen-diluted mixture and 0.2 atm for the argon-diluted mixture [40]. The right boundary was defined as an open pressure outlet, while the other boundaries were set as walls.

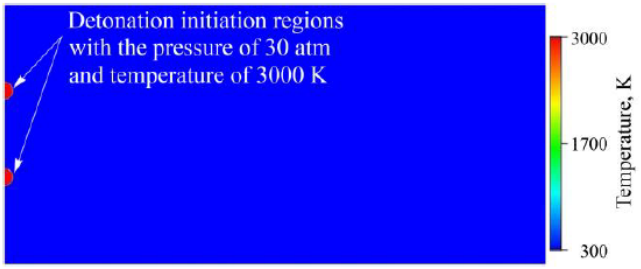

Figure 4.4 - Temperature distribution and initiation regions [40].

In the second stage of the study, a spin detonation was simulated using a 20 mm x 70 mm long 2D domain, with detonation initiated by a 20 mm x 1 mm high-energy region set to a pressure of 30 atm and a temperature of 3000 K [40]. When the detonation wave was a distance of 5 mm away from the right boundary, the walls were then switched to periodic boundary walls, enabling continuous wave propagation. The upper boundary of the domain was set as an open outlet at 1 atm, while the lower boundary acted as a fixed mass flow inlet for the premixed hydrogen-oxygen mixture with a temperature of 300 K [40]. The stoichiometric mixture of hydrogen and oxygen were supplied, with a species mass fraction of 0.1111 and 0.8889 [40].

The results showed that the calculated detonation velocities were consistently lower than the ideal CJ detonation velocities, which is expected for spin detonation. The specific impulse of the combustion chamber was calculated to be 17% higher than that of a conventional liquid-propellant rocket engine (LPRE) [40]. This result highlights the efficiency benefits of CSD. However, the authors noted that more accurate results could be obtained through three-dimensional simulations that account for the actual geometry of the injection and supply systems. However, with the 2D simulational, they were indeed able to observe the spinning and propagation of detonation waves.

4.1.4 Examination of Wave Speed Using Simplified CFD Article

This study implemented a two-dimensional simulation of an RDE, specifically using a reactive Euler solver to model it, while also employing a quasi-2D framework [41]. Their main goal was to determine some of the causes of low detonation wave propagation speeds, which is a trend seen with many other studies conducted. Premixed gas of hydrogen and air is set to be a single, calorically perfect, characterized by a specific heat ratio of 1.264, a real gas constant of 73.92 ft-lbf/lbm/R, and a fuel heating value of 51,571 BTU/lbm [41]. The reaction model was simplified using a user-defined reaction rate proportional to the density and reactant mass fraction, without an Arrhenius temperature dependence. The reaction was permitted only above a threshold temperature, set to 2.5 times the reference temperature.

For temporal integration, the simulation used an explicit, second-order, two-step, Runge-Kutta method, while spatial flux derivatives were calculated using Roe's Riemann solver [41]. Second-order spatial accuracy was achieved using the MUSCL scheme, and oscillations were controlled using slope limiters, while the fluid properties were normalized using reference values of pressure of 14.7 psia, density of 0.055 lbm/ft^3, temperature of 520 R, and sound speed of 1250 ft/s, which simplified numerical calculations [41]. The influence of skin friction and heat transfer was neglected in this study to focus solely on the detonation dynamics.

The fuel and oxidizer were introduced into the RDE isentropically through the inlet, provided that the pressure inside the RDE remained below the manifold pressure of 8 atm [41]. To prevent backflow during high-pressure conditions behind the detonation front, a notional valve model was used. The azimuthal inlet velocity was iteratively adjusted to achieve a stable detonation wave, making the simulation domain time-invariant. The stoichiometric hydrogen-air mixture was supplied at an inlet manifold temperature of 536 R, and the static pressure at the outlet was set to 1 atm [41]. To simulate a continuous detonation wave, the left and right boundary conditions were set to be symmetric. The computational grid consisted of 400 cells by 80 cells in the axial direction, with a non-dimensional time step of 5.0 x 10^-5 [41].

Despite the simplified setup, the model was able to reproduce several critical phenomena observed in experimental RDEs. These included reduced wave speeds, ranging from 15% to 40% lower than the ideal Chapman-Jouguet speed, and lower peak temperatures due to turbulence-induced thickening of the reaction zone [41]. The study ultimately concluded that while the reduced detonation wave speed was notable, it did not significantly affect the overall performance of the idealized RDE as measured by gross specific impulse.

4.1.5 2D Simulation of Detonation Wave Propagation in RDE Article

This study focused on evaluating a 2D simulation of an annular RDE using ANSYS Fluent. The original 3D geometry featured a cylindrical combustor with an inner diameter of 90 mm, an outer

diameter of 100 mm, and a length of 75 mm. However, for computational efficiency, this 3D model was transformed into a 2D "unrolled" configuration, effectively representing the annular chamber as a rectangular domain [42].

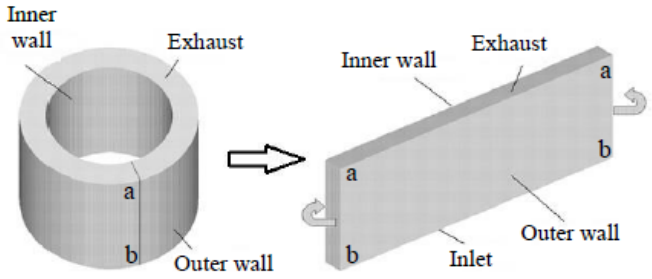

Figure 4.5 - 3D to 2D conversion geometry [42].

The simulation setup began with a structured orthogonal mesh composed of quadrilateral elements, with a uniform cell size of 0.5 mm × 0.5 mm. The reactants, a stoichiometric hydrogen-air mixture, were injected at an initial pressure of 1.7 bar and a temperature of 300 K [42]. The inlet was configured as a continuous flow boundary, using a User Defined Function (UDF) to maintain constant stagnation properties. This UDF dynamically adjusted the reactant velocity based on the local pressure of the adjacent cells, allowing the inlet to operate under three conditions: no injection, subsonic injection, and sonic injection [42].

The outlet of the domain was defined as a pressure outlet, maintaining a constant static pressure of 11 kPa to match experimental conditions. Initially, the left and right boundaries of the chamber were treated as walls to prevent unwanted wave reflections. Once the detonation wave was established and began propagating, these wall boundaries were replaced with periodic boundaries. This adjustment enabled the wave to propagate continuously without encountering reflective interference [42].

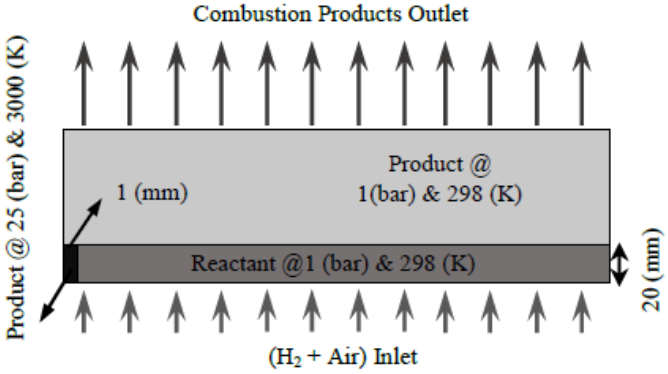

Figure 4.6 - Regions and ignition strategy [42].

The simulations were carried out using an unsteady, density-based, finite volume solver in ANSYS Fluent. They also utilized an Euler-based solution approach, focusing exclusively on gas

dynamic properties within the combustion chamber. Temporal discretization was performed using a second-order implicit scheme, while spatial discretization employed a second-order upwind approach [42].

The detonation was initiated using a specific region located at the left-bottom corner of the domain. This ignition region was defined with a high temperature of 3000 K and a pressure of 10 bar [42]. The combustion process was modeled using a one-step irreversible Arrhenius reaction model for the hydrogen-air mixture. The reaction kinetics were defined by the following parameter specific heat ratio of 1.29 universal gas constant 368.9 J/kg·K, pre-exponential factor of 7.5×10^9 s^-1, and an activation energy of 4.794×10^6 J/kg [42].

From their simulations, the test with an equivalence ratio of 1 was able to achieve a detonation wave velocity of 1250 m/s, a static temperature of 3271 K, and a static pressure of 20.29 bar [42]. These values represented the highest performance metrics when compared to other tested equivalence ratios of 0.8 and 1.2. The results demonstrated the model's ability to effectively capture critical detonation wave characteristics in a 2D setup, validating the approach used.

4.1.6 Feasibility and Performance with Ammonia/Hydrogen/Air Article

This study implemented a 2D simulation of an RDE to investigate the feasibility and performance with a premixed ammonia/hydrogen/air, using a detailed chemical reaction mechanism consisting of 19 species and 80 reactions [43]. The main objectives were to assess the impact of varying equivalence ratios and injection temperatures on detonation wave propagation, pressure gain performance, and NOx. OpenFOAM was selected as the simulation software, with the RYrhoCentralFoam solver, which is a density-based, multi-component, reactive solver capable of handling high-speed compressible flows [43]. The governing equations included conservation of mass, momentum, energy, and species mass fraction, along with the ideal gas equation of state. A second-order implicit backward scheme for time integration was used, and the Total Variation Diminishing (TVD) scheme for energy and species transport equations [43]. A van Leer limiter was applied to maintain numerical stability.

The computational setup featured a simplified 2D rectangular model representing an unwrapped annular RDE combustion chamber. The domain measured 0.3 meters in length and 0.12 meters in height, and it was discretized using a uniform Cartesian grid consisting of 900,000 cells, 1500 x 600, with a grid size of 0.2 mm × 0.2 mm [43]. The ignition zone was located at the lower left corner of the domain, with a size of 0.02 m × 0.03 m, and was initialized with a temperature and pressure that is consistent with a one-dimensional detonation wave profile [43]. The prefilled region was set to a height of 0.03 m and a pressure of 2 atm.

For boundary conditions, the premixed mixture was injected from the inlet under isentropic conditions, while the outlet featured non-reflective boundary conditions based on local Mach numbers to prevent wave reflections [43]. The lateral boundaries were set as periodic to simulate continuous wave propagation, while the back pressure at the outlet was maintained at 1 atm. The injection pressure was set at 0.4 MPa, with the injection temperature varying between 400 K and 1000 K to evaluate performance under different air-breathing conditions [43].

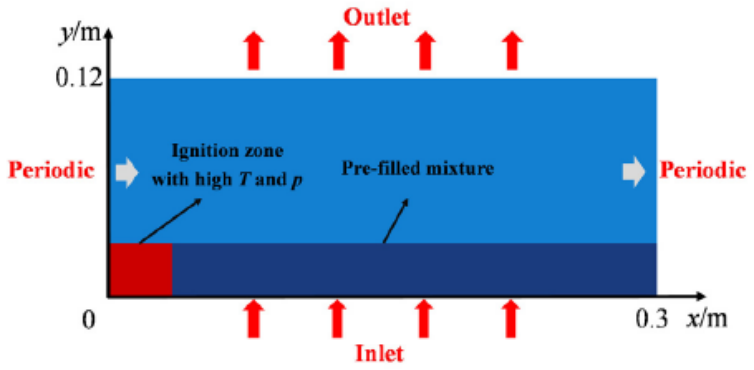

Figure 4.7 - Computational domain and boundary conditions [43].

A grid sensitivity study was conducted, testing multiple grid sizes to ensure accurate resolution of the detonation wave. The final grid size of 0.2 mm × 0.2 mm was selected for its balance between computational efficiency and numerical accuracy. At this resolution, the detonation front height was measured at 0.0389 m, and the wave speed was 1787.1 m/s, with a percent error of 0.16% when compared to theoretical values, and the temperature and pressure deviation had percent errors of 0.70% and 1.23% [43].

Overall, the primary focus of the study was to observe the effects of injection total temperature and ammonia concentration on the RDE's performance. The simulations provided a comprehensive analysis of the detonation wave propagation, including the formation of a propagation map that illustrated the stability and behavior of the detonation waves under various conditions. Key performance metrics were assessed, including the RDE's flow field structure, detonation height, wave propagation speed, pressure gain performance, and NOx emissions [43]. Based on the simulation results, several important conclusions were drawn, providing valuable insights into the operational characteristics of the NH3/H2/air RDE and its potential for practical applications.

4.1.7 Numerical Investigation of Species Transport Article

This study investigated the impact of thermal radiation in the simulation of turbulent, non-premixed combustion using multiple fuel and oxidizer mixtures within a 2D cylindrical combustion chamber [44]. The primary objective was to evaluate the emission characteristics

and thermal performance of various fuels, including diesel, hydrogen, kerosene, n-butanol, pentane, propane, and methane, while exploring potential strategies to minimize emissions. The simulation was conducted using ANSYS Fluent, with the standard k-ε turbulence model employed for turbulence closure, and was configured using a steady-state, pressure-based solver with an absolute velocity formulation [44].

The cylindrical combustion chamber had a diameter of 45.0 cm and a length of 180.0 cm.The chamber walls were defined as smooth, with a no-slip boundary condition to ensure realistic interaction between the flow and solid surfaces [44]. Fuel was introduced through a small nozzle located at the center of the chamber's inlet, while air entered the chamber at a larger inlet positioned around the fuel nozzle. The fuel inlet had a diameter of 0.5 cm, while the air inlet had a diameter of 22.5 cm. The fuel was injected at an initial velocity of 80.0 m/s and a temperature of 300 K, while the air entered at a velocity of 0.5 m/s and the same temperature [44]. Species transport was enabled to account for the combustion of various fuels, with the flame modeled as a turbulent diffusion flame.

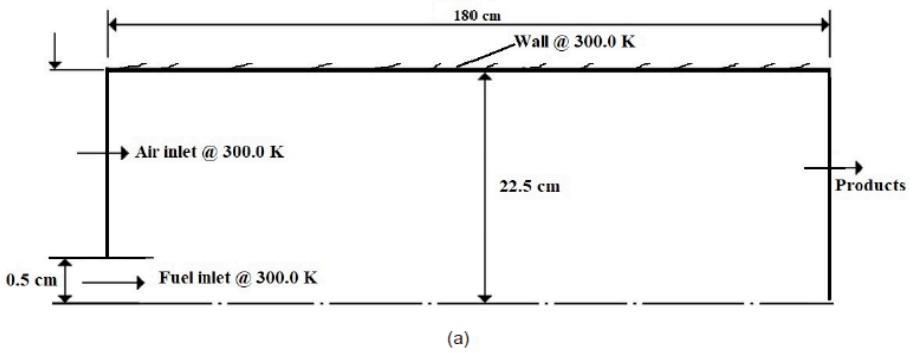

Figure 4.8 - Input and output from combustion chamber [44].

The CFD analysis focused on evaluating combustion characteristics, including temperature distribution, NOx emissions, CO2 concentrations, and O2 and H2O levels at the combustion chamber outlet. Area-weighted average velocity, mass-weighted average temperature, and mass fraction of species at the outlet were calculated to provide detailed insights into the combustion performance of each fuel. Overall, the study demonstrated the importance of fuel selection and combustion chamber design in controlling emissions and optimizing combustion efficiency, providing valuable insights for future combustion chamber design and fuel selection strategies.

4.1.8 Investigation of Detonation Theory and CRDE Article

This study, conducted by Samuel Zunigo from San Jose State University, focused on the numerical simulation of continuous rotating detonation engines (CRDEs) using a

two-dimensional configuration. The investigation primarily centered on the simulation of a one-step hydrogen-air reaction model, exploring both ideal and non-ideal injection conditions to understand their effects on detonation wave stability and performance.

The simulation was performed using ANSYS Fluent with a density-based solver, the simplified unsteady Euler equations, axis symmetric, laminar, and transient, neglecting transport properties like viscosity, thermal conduction, and mass diffusion [45]. ROE's flux difference splitting scheme was set, along with a second-order implicit scheme for the temporal discretization with a constant time step of 1 x 10^7 s, and a spatial discretization set to a second order upwind scheme and a courant number of 0.5 [45]. Turbulence was also omitted to further reduce computational complexity. The chemical model was based on a one-step, irreversible Arrhenius reaction for hydrogen and air, characterized by constant thermodynamic properties for simplicity. The model was configured as a two-dimensional axisymmetric domain, with a uniform structured mesh of 0.1 mm spacing.

The boundary conditions were defined as adiabatic walls for most of the domain, with the exception of the bottom boundary, which was set to symmetry, and the right boundary, which was defined as a pressure outlet at standard atmospheric conditions. The initial conditions were divided into two regions: the burned gas region, ignition zone, and the unburned gas region. In the burned gas region, the initial temperature was set to 3500 K and the pressure to 90 atm, with mass fractions of 0.25480 for water and 0.74520 for nitrogen [45]. In contrast, the unburned gas region was initialized with a temperature of 300 K, a pressure of 1 atm, and species mass fractions of 0.02852 for hydrogen, 0.22640 for oxygen, and 0.74510 for nitrogen [45]. A thin region of burned gases was patched at the left end of the domain to initiate the detonation wave, while the remaining region contained the unburned stoichiometric hydrogen-air mixture. This can be seen down below.

Figure 4.9 - Patch sections for tube [45].

From the simulation results, a stable propagating combustion wave was successfully generated, as indicated by the pressure and temperature contours. When the numerical results were compared to theoretical values, they consisted of a 6.49% difference for pressure, a 5.72% difference for temperature, and a 2.36% difference for detonation velocity [45]. These minor discrepancies confirmed that ANSYS Fluent could accurately simulate both ZND and CJ conditions using a simplified, stoichiometric one-step hydrogen-air chemical mechanism.

This study also explored two different injection models for the CRDE: an ideal injection model using a UDF and a non-ideal injection model with multiple injectors distributed across the chamber, modeled after a benchmark study to provide comparative results. The non-ideal injection model featured multiple discrete injectors along the chamber, each delivering a stoichiometric hydrogen-air mixture at 10 atm and 300 K [45]. The combustion chamber itself was initialized with air at atmospheric conditions, while the inlet operated as a velocity inlet. However, this model encountered significant stability issues. As the detonation wave propagated, a back pressure developed behind the wave, disrupting the injector operation. This led to excessive pressure buildup, causing solver divergence and eventual simulation failure.

In contrast, the ideal injection model used a UDF to dynamically control the inlet boundary conditions. This UDF allowed the inlet to adapt between three possible states: no flow, subsonic injection, and supersonic injection, based on the local wall pressure [45]. The adaptive control provided by the UDF improved stability by maintaining proper injection conditions. Despite this enhancement, the UDF approach also faced implementation challenges in ANSYS Fluent, with persistent debugging issues preventing full functionality.

4.1.9 Potential Scalability for Use in Non-Rocket Based Applications Article

This study, conducted by Ian Vaca as part of his master's project at San Jose State University, aimed to conduct an extensive literature review on RDEs and explore their potential scalability for non-rocket applications. To achieve this, Vaca based his computational model heavily on the work of Samuel Zunigo, replicating their setup while focusing on varying the engine size to assess performance parameters.

Vaca also adopted the UDF developed by Zunigo to model the ideal injection conditions. The initial conditions for the velocity inlet in his simulation were set with a velocity of 317 m/s, a temperature of 250 K, a supersonic initial gauge pressure of 535,282 Pa, and an outflow gauge pressure of 101,325 Pa [46]. For the pressure outlet, the gauge pressure was set to 0 Pa, with a Mach number of 0.6.

For the solution methods, Vaca utilized an implicit formulation with the Roe-FDS flux type, and spatial discretization was set to least squares cell-based for gradients and second order upwind for flow [46]. The initial courant Number was set to 0.05, ensuring numerical stability during the early stages of the simulation. Despite the similarity to Zunigo's setup, Vaca observed that the simulation did not capture the CJ detonation wave as expected. The absence of the CJ wave, which should be clearly visible in the simulation results, indicated a potential issue with the numerical configuration or boundary conditions, prompting further investigation.

4.2 2D Implementation on Numerical Setup

With the completion of the literature review, the next step is to determine the most effective approach for modeling a two-dimensional combustion chamber geometry for this project. This selection will also establish benchmark results, which will serve as a basis for an accurate comparison. Key trends observed across the reviewed studies, including initial conditions, fuel and oxidizer choices, computational physics setup, solution models, and boundary conditions, will guide the final model configuration.

4.3 Comparative Analysis

ANSYS Fluent was found to be the most commonly used CFD software, followed by OpenFOAM and other custom solvers. Majority of the studies conducted there simulations with a 2D rectangular or unrolled annular geometry of varying lengths and widths, with mesh resolutions ranging from 0.1 mm to 0.5 mm. The most frequently used fuel and oxidizer was hydrogen and air. For the boundary conditions, the inlet was typically assigned either a velocity inlet or a mass flow inlet and the outlet was assigned a pressure outlet. Initial conditions consisted of a temperature of 300 K and a pressure of 1 atm. For a majority of the studies, the walls were changed to periodic walls as soon as a detonation wave was observed. This would allow for the simulation of a propagating rotating detonation wave. The governing equations that were modeled were either the Euler or RANS models, with FRC and species transport for combustion modeling. There were two main types of ignition strategies, first of which being direct ignition, high-energy regions, and the other utilizing a UDF-controlled inlets.

With this analysis done, the steps for the numerical simulation and the CFD set up can now be further discussed with the specific implementations from the articles investigated in this literature review.

Chapter 5: Steps for Numerical Analysis & CFD Set-up

5.1 Simulation Framework

ANSYS Fluent will be used as the primary CFD software for conducting the simulations and evaluating performance metrics, as this was the most commonly used software in the articles researched. It was noted that the most simplified 2D simulations were done using Ansys Fluent, as this software is able to support the computational complexity required for detonation wave modeling. This software consistently demonstrated the ability to accurately capture critical detonation phenomena, making it a reliable choice for the current project's simulation framework. The next couple of sections will go into depth for each step of the numerical setup. This will include geometry, mesh, models, boundary conditions, solution monitors, and physics.

5.2 Geometry Set-up and Mesh

The initial step in the setup process involves creating the geometry in ANSYS SpaceClaim. Given that the project aims to simulate an unrolled 2D annular geometry, the geometric representation will be a simple rectangle. However, despite its simplicity, this geometry is critical because it directly correlates with the chamber length and radius of the equivalent three-dimensional annular combustion chamber. This conceptualization can be seen in Farahani and Badrgoltapeh's numerical work [42]. They show a clear conversion from 3D to 2D geometry, with the dimensions given. For the first case, the dimensions will be replicated to provide a realistic approximation, if in the future, 3D simulations would be conducted. The dimensions for the 1 case can be seen in Table 5.1. For the second case, the height was increased to observe how changing the geometry affects the propagation of the detonation wave, as well as the structure.

Table 5.1 - Dimensions of geometric variations.

Case Number	Length (mm)	Height (mm)
1	300	75
2	300	125

For the setup of the mesh, the first step is to define the boundary condition using the named selection. The bottom horizontal line was assigned the inlet while the top was assigned the outlet. The left and right vertical lines are assigned as walls. The mesh sizes used in the reviewed articles ranged from 0.1 x 0.1 mm to 0.5 x 0.5 mm. Some studies even conducted mesh sensitivity analyses, which showed that finer meshes provided slightly improved accuracy in capturing detonation waves and shock structures. However, the increase in computational cost

with finer mesh sizes was significant, while the improvement in numerical accuracy was minimal. In order to provide a simplistic model with the appropriate computational power available for this project, a 0.5 mm uniform quadrilateral mesh was chosen, making a total of 90,000 cells, which can be seen down below.

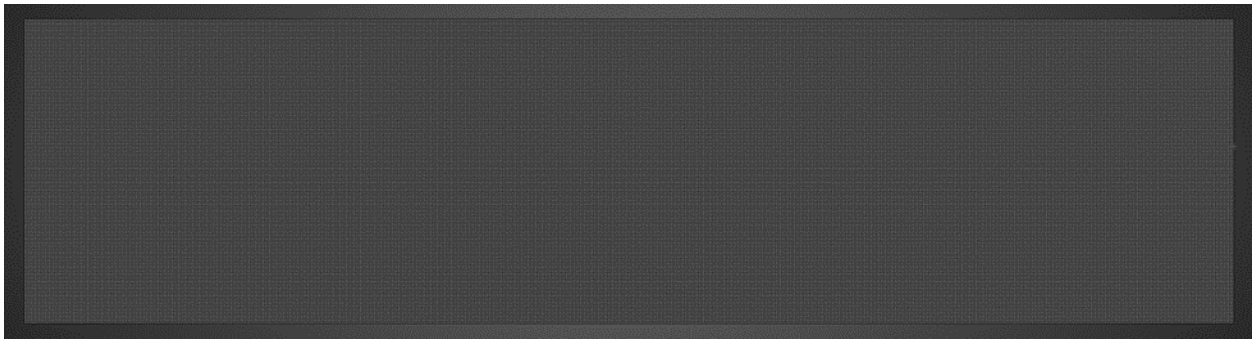

Figure 5.1 - Mesh.

5.3 Set up of Model

To achieve a simplified 2D RDE simulation setup, a standardized approach is implemented. This was done by examining the trends identified in the literature review of 2D CFD studies. Many of these studies exhibited consistent model configurations, which have been carefully analyzed and selected for this project. The general model configuration will begin with the selection of a 2D planar, density-based, transient model with an absolute velocity formulation. The energy equation will be activated for all models to ensure that thermal effects, including temperature changes and heat release due to combustion, are accurately represented. The inviscid model was selected to model the reduced Euler equations, which improves the computational complexity and time. This simplification is also appropriate for detonation modeling, where the transport properties including thermal conductivity, viscosity, and mass diffusion can be neglected.

The species transport model is enabled to allow for the simulation of the chemical reactions within the combustion chamber, specifically focusing on the one-step hydrogen-air reaction mechanism, which is selected directly from the ANSYS Fluent database. Although many studies in the literature review utilized a detailed chemical mechanism with multiple species and reactions to enhance combustion accuracy, these were typically imported or manually defined. This approach allowed for precise control over critical parameters such as activation energy and thermodynamic properties. Initially, this project aimed to replicate that approach by importing a detailed chemical mechanism. However, there were many technical issues with importing the mechanism and thermodynamic data which led to the majority of the files and data being corrupted and unusable. As a result, the default one-step hydrogen-air reaction mechanism provided by ANSYS Fluent will be used. This decision allows for a unique aspect to the current

study, as none of the reviewed articles explicitly utilized this default mechanism. This will help with observing how this simplified model affects simulation results.

Volumetric reactions are activated to ensure that chemical reactions occur throughout the domain where the fuel and oxidizer interact. The stiff chemistry solver is selected, which is critical for handling the rapid reaction rates associated with detonation chemistry, which helps prevent numerical instability. Direct integration is chosen for the integration parameters as this offers a more accurate calculation of the reaction rates without the need for iterative convergence. For turbulence-chemistry interaction, the Finite-Rate/No TCI option is selected. This setting is chosen by default because it allows the simulation to focus on the chemical kinetics of detonation without adding the complexity of turbulence-chemistry interaction models.

5.4 Materials and Mixture

To accurately model the properties of hydrogen and air in the RDE simulation, it is essential to ensure that the mixture species are correctly defined. For the species order, nitrogen is listed as the last species in the mixture definition. This is important because nitrogen is treated as an inert gas and is the most abundant species in the air. The density model is set to ideal gas, which is critical for accurately capturing the compressible flow behavior of the detonation process. All other thermodynamic properties of the species such as specific heat, thermal conductivity, standard state enthalpy and entropy are left at their default settings provided by the ANSYS Fluent database. This maintains consistency with the standard property values for hydrogen, oxygen, and nitrogen.

5.5 Boundary Conditions

For the boundary conditions of the 2D RDE simulation, the inlet was initially assigned as a velocity inlet. However, upon reviewing the literature, it was observed that most studies utilized either a velocity inlet with a UDF or a mass flow inlet. The UDF offers a more realistic representation of the injection model However, the complexity of creating and debugging the UDF code led to persistent issues which prevented a successful implementation. As an alternative, various velocity values were tested, but the simulations only displayed deflagration rather than a stable detonation wave. To address this, a mass flow inlet with a mass flux of 357 kg/m^2s was selected, consistent with the setup from the first article in the 2D literature review [38]. This adjustment proved effective, as the simulation began to exhibit a stable detonation wave, demonstrating significant improvement. The decision to use a mass flow inlet ensures reliable and consistent inlet conditions while aligning with validated methods from the literature.

Standard atmospheric conditions were assigned for the simulation, with the inlet temperature set to 300 K and the pressure to 1 atm. To maintain a stoichiometric hydrogen-air mixture with an

equivalence ratio of 1, species mass fractions were carefully defined, replicating the values used in the first article reviewed [38]. This approach was selected because it aligns with the default mixture configuration in ANSYS Fluent, simplifying the chemical setup. Typically, imported chemical mechanisms involve complex reaction networks with 10 to 20 species and numerous reactions, resulting in a wide range of product species. However, the first article presented a more streamlined set of species mass fractions, effectively capturing the essential combustion dynamics without the complexity of extensive chemical kinetics [38]. This simplified configuration was directly implemented to ensure consistency and facilitate accurate comparison of results. Both the inlet and outlet conditions were configured using these species mass fractions, with the inlet reflecting the reactant mixture and the outlet representing the product composition. At the outlet, a pressure outlet condition was set with a gauge pressure of 100000 Pa, while the backflow temperature was maintained at 300 K.

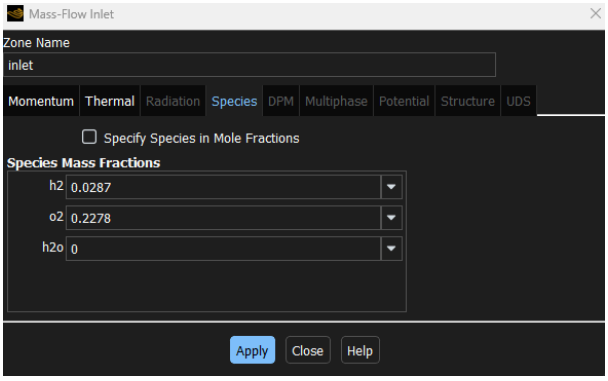

Figure 5.2 - Species reactant mass fraction at inlet.

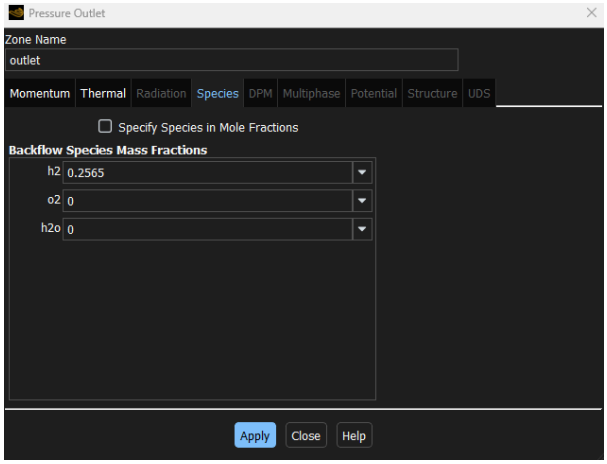

Figure 5.3 - Species product mass fraction at outlet.

One of the most critical aspects of this setup was the treatment of the wall boundaries. Initially, the walls were configured as non-slip adiabatic walls, to prevent any heat transfer or fluid motion at the surface. This setup allows the detonation wave to propagate within the combustion

chamber without interference. However, once the detonation wave travels the full length of the chamber, the walls are then switched to periodic boundaries. This transition enables the detonation wave to propagate continuously, which effectively simulates a rotating detonation wave without any artificial reflection or termination. This method allows for a stable, self-sustaining detonation wave to be simulated in a two-dimensional geometry, closely replicating the behavior of a 3D rotating detonation engine.

However, initial simulation results revealed a critical challenge. Due to the inlet being defined as a mass flow inlet, the detonation wave began to dissipate once it crossed the periodic boundary and re-entered the domain. This dissipation prevented the formation of a stable rotating detonation wave. A potential solution to this issue is the implementation of the UDF for the velocity inlet. A UDF would allow for dynamic control of the inlet velocity, maintaining a consistent flow rate that aligns with the detonation wave dynamics. This modification could significantly enhance the simulation's ability to capture an accurate, stable rotating detonation wave. However, persistent difficulties in developing a functional UDF have prevented this approach. Therefore, the simulation setup has been adjusted to maintain fixed wall boundaries rather than periodic walls, effectively transforming the configuration into a shock tube model. This adjustment enables the observation of a singular propagating detonation wave rather than a continuous rotating wave. While this setup may differ from the intended rotating detonation model, it still provides valuable insights by capturing the fundamental detonation wave dynamics, offering sufficient data for detailed analysis.

5.6 Ignition

For the ignition method, a cell register region was defined within the domain, measuring 0.005 m x 0.02 m in the bottom left corner, as seen in the figure below. This region was patched with an initial temperature of 3500 K and a pressure of 30 bar, consistent with the conditions applied in the first article of the 2D literature review [38]. Most of the reviewed studies employed a high-energy ignition region, with temperatures typically exceeding 3000 K and pressures significantly above atmospheric levels. Some studies further enhanced ignition by assigning a high initial velocity within this region. The use of high temperature and pressure ensures rapid energy release, effectively initiating the combustion process and triggering a detonation wave. This localized ignition approach is designed to achieve stable detonation wave propagation across the combustion chamber, closely replicating the direct ignition mechanism used in many experimental RDE setups. By maintaining consistency with the literature, this method provides a reliable and validated means of initiating detonation.

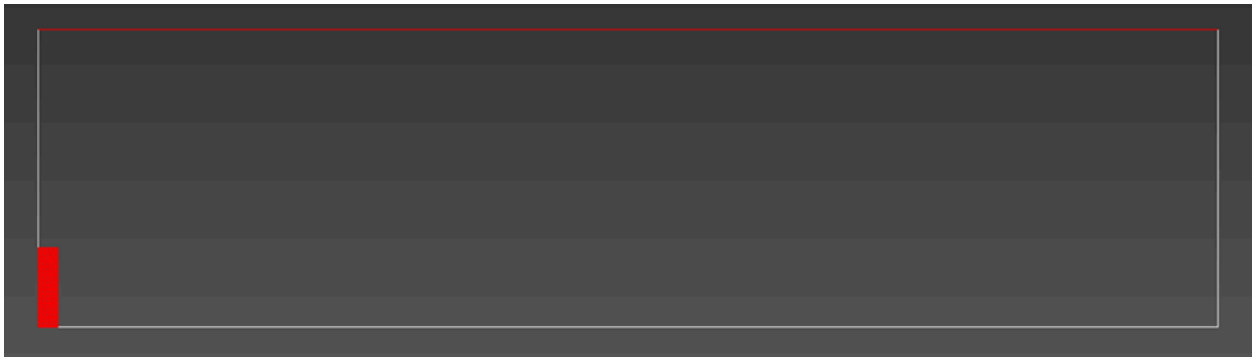

Figure 5.4 - Ignition zone.

5.7 Method, Controls, & Initialization

For the solution methods, an implicit formulation was selected to ensure numerical stability during transient calculations. The flux type was set to Roe-FDS, which is used to accurately capture shock wave interactions and detonation wave propagation. Spatial discretization was defined using a least-squares cell-based gradient method, ensuring accurate gradient calculation across the mesh. For the flow equations, a second-order upwind scheme was applied, providing improved numerical accuracy by considering upstream conditions. Temporal discretization was managed using an implicit first-order transient formulation, providing a balance between computational efficiency and solution accuracy. For the simulation controls, a courant number of 0.5 was chosen as it was informed by the findings of the literature review, which demonstrated that a lower courant number improves numerical stability and accuracy in detonation wave simulations.

The simulation utilized a hybrid initialization. For the run calculation settings, the simulation was configured with 180 time steps, a time step size of 1e-06 seconds, a maximum of 50 iterations per time step, and a reporting interval set to 1.

Chapter 6: Results and Discussion

6.1 First Case

6.1.1 Pressure, Temperature, & Velocity Contours

The pressure, temperature, and velocity contours are provided below in intervals of 20 time steps to observe the detonation wave traveling through the chamber. By analyzing the pressure contours, it is clear that the detonation wave initiates with a high-pressure front, but gradually dissipates as it travels the length of the chamber. The reduction in pressure indicates a loss of wave strength. This suggests that the simulated detonation wave may be transitioning to a deflagration wave rather than sustaining a stable and propagating detonation wave.

The temperature contours further confirms this observation, as a decrease in temperature along the wave propagation path can be seen. While the initial ignition region displays a high temperature, the energy quickly dissipates, which leads to a weakened thermal profile. This behavior could possibly indicate that the ignition energy is not sufficient enough to sustain a stable detonation wave or that the mass flow rate is not providing enough reactants to support continuous combustion.

The velocity contours show a consistent flow pattern, but the peak velocity values decrease over time. This reduction in velocity aligns with the pressure and temperature profiles, further indicating wave dissipation. The wavefront lacks the sharp definition characteristic of a strong, stable detonation wave, suggesting that the simulation is not fully capturing the high-speed propagation expected in an RDE.

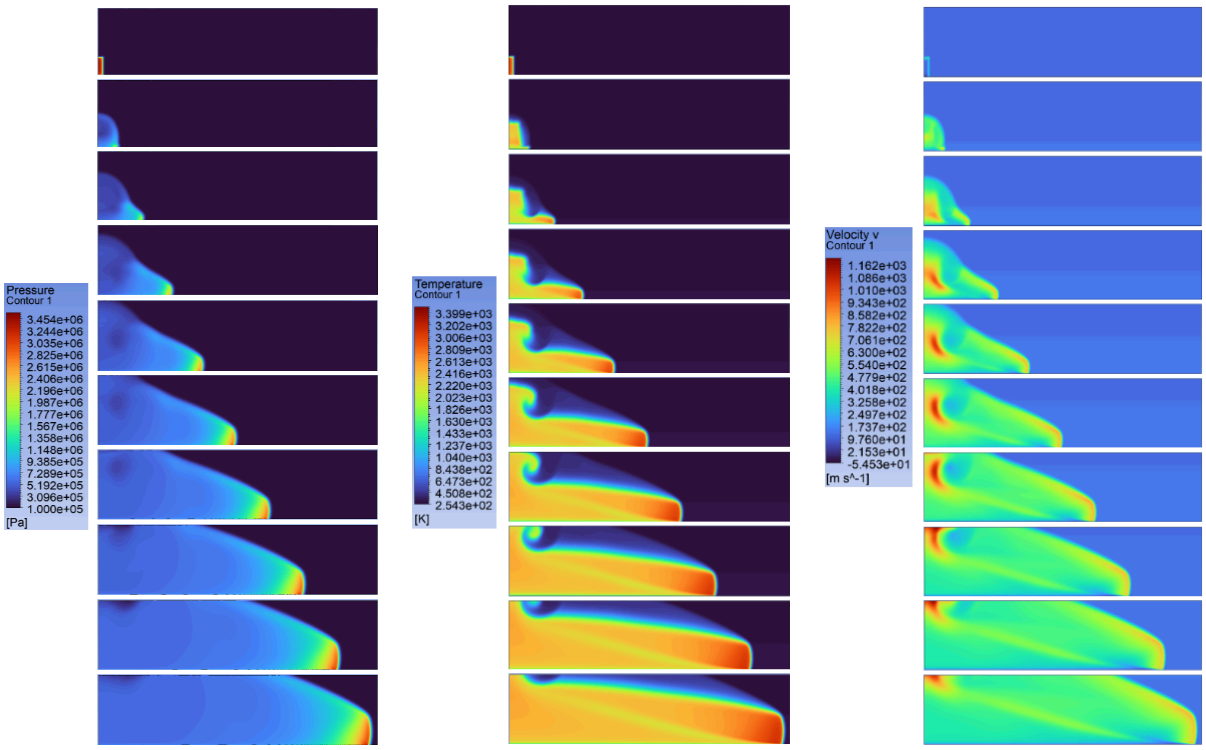

Figure 6.1 - Pressure, temperature, and velocity contours in intervals of 20 time steps.

6.1.2 Analysis of Minimum and Maximum Values

Table 6.1 presents the minimum and maximum values recorded from the pressure, temperature, and velocity contours. The maximum pressure of 3.56E+06 Pa is significantly higher than the expected CJ pressure for hydrogen-air detonation, indicating that the initial ignition may be generating an excessive pressure spike. However, the minimum pressure of 100,000 Pa (1 atm) is consistent with atmospheric conditions, which suggests that the simulation is correctly maintaining the boundary conditions.

The maximum temperature of 3496.93 K is close to the expected CJ temperature, indicating that the simulation is effectively achieving high-temperature combustion. However, the minimum temperature of 254.254 K is unusually low, which may indicate unintended cooling effects, possibly due to boundary interactions or insufficient energy input in the ignition region.

Velocity values range from -54.5282 m/s to 1200.5 m/s. The maximum velocity of 1200.5 m/s is slightly higher than the theoretical CJ velocity for hydrogen-air, which is approximately 1089.2 m/s. The negative velocity values may indicate backflow or incorrect boundary configuration, which could be disrupting the wave propagation.

Table 6.1 - Minimum and maximum values recorded from contours.

Minimum Pressure (Pa)	Maximum Pressure (Pa)	Minimum Temperature (K)	Maximum Temperature (K)	Minimum Velocity (m/s)	Maximum Velocity (m/s)
100000	3.56E+06	254.254	3496.93	-54.5282	1200.5

These results further highlight the need for refinement in the simulation setup, including optimization of the ignition region, adjustment of mass flow rates, and careful examination of boundary conditions to prevent wave dissipation. However, to accurately verify the suspected issues with detonation wave generation and propagation, a line probe was strategically placed along the wave front. This probe was used to extract critical data, capturing the pressure, temperature, and velocity characteristics of the wave. The extracted data is presented in the following plots, providing a clear representation of the wave's behavior, which will then be compared to benchmarked data obtained from NASA CEA code.

6.1.3 Experimental CJ Parameters

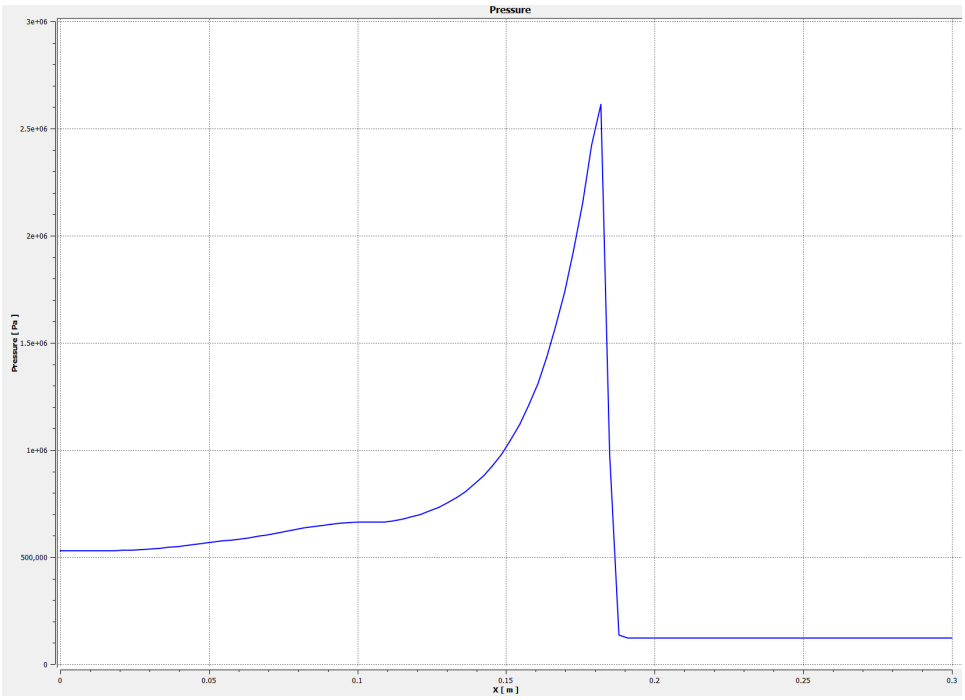

Figure 6.2 - CJ Pressure plot.

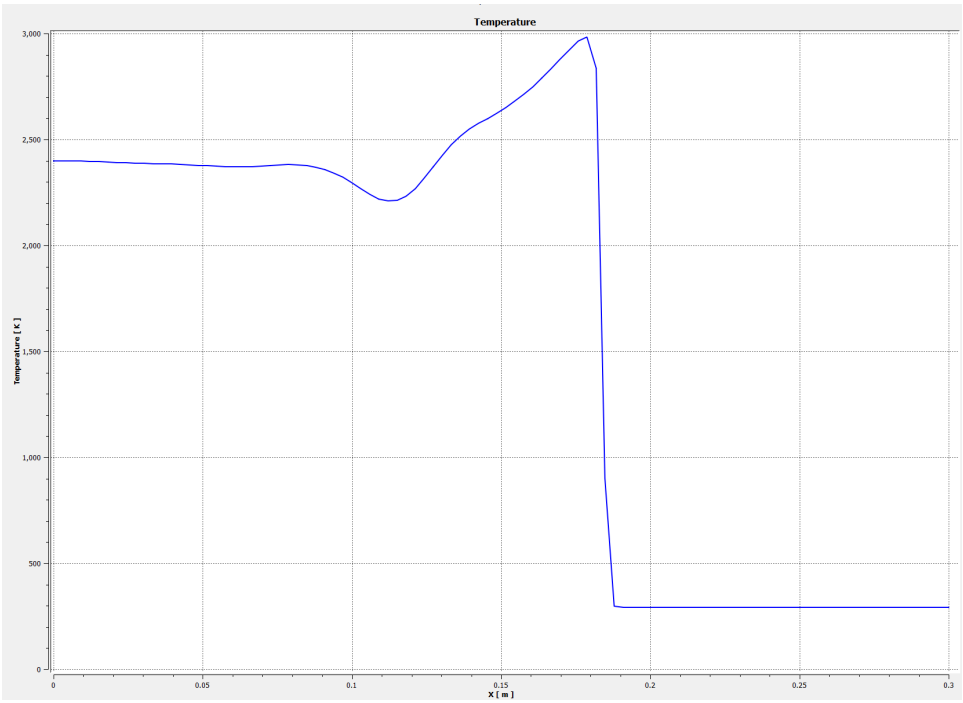

Figure 6.3 - CJ Temperature plot.

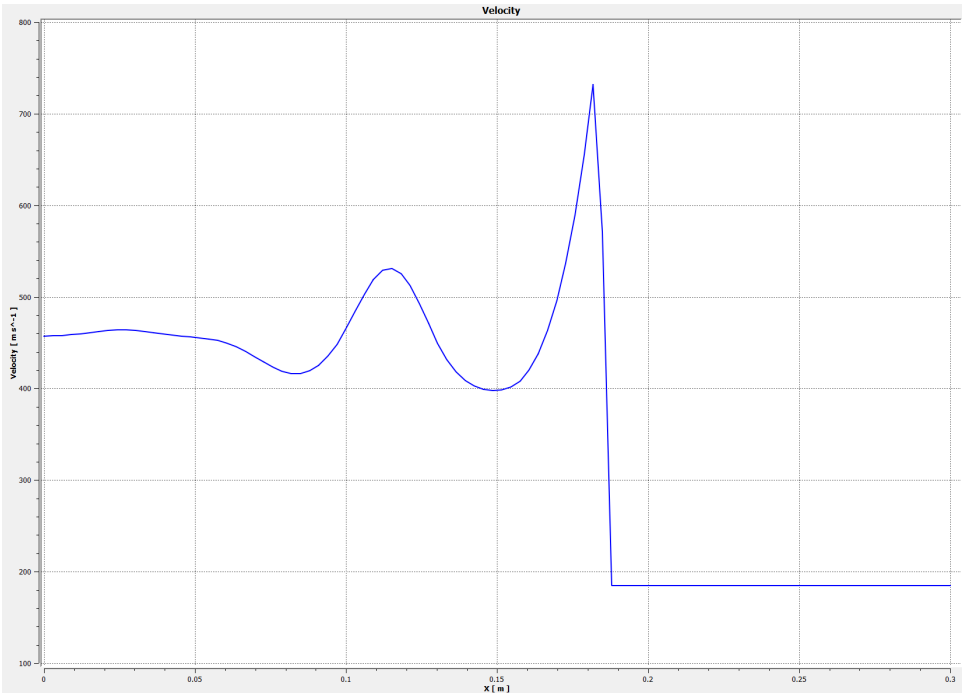

Figure 6.4 - CJ Velocity plot.

Table 6.2 presents a benchmark comparison between the simulation results and the theoretical CJ values obtained from NASA CEA. The experimental CJ temperature of 2943.85 K closely aligns with the theoretical value, resulting in a minimal percent error of 1.81%. This agreement suggests that the simulation effectively captures the high-temperature characteristics of the detonation wave, likely due to accurate combustion modeling.

However, the experimental CJ pressure of 2,600,000 Pa significantly exceeds the theoretical value of 1,569,600 Pa, resulting in a high percent error of 65.65%. This discrepancy indicates that the simulated pressure is experiencing an excessive initial spike, potentially caused by the high-energy ignition region. It is noted that over-pressurization is common in simulations where the ignition energy is not carefully controlled.

The experimental CJ velocity of 740 m/s is notably lower than the theoretical value of 1,089.2 m/s, leading to a percent error of 47.23%. This discrepancy may be attributed to wave dissipation, inadequate reactant supply, or boundary condition effects that reduce the wave speed. The lower velocity confirms that the simulated wave is transitioning towards a deflagration wave rather than a detonation wave.

Table 6.2 - Benchmark comparison to experimental data.

Experimental CJ Temperature (K)	Theoretical CJ Temperature (K)	Percent Error %	Experimental CJ Pressure (Pa)	Theoretical CJ Pressure (Pa)	Percent Error %	Experimental CJ Velocity (m/s)	Theoretical CJ Velocity (m/s)	Percent Error %
c	2943.85	1.81%	2,600,000	1,569,600	65.65%	740	1089.2	47.23%

6.2 Results of Second Case

The second case was simulated following the same numerical setup, boundary conditions, and ignition strategy as the first case. This approach ensures consistency in the analysis, allowing for a direct comparison of results between the two cases. The same methodology was applied to extract key performance metrics, including pressure, temperature, and velocity at the detonation wave front. The following sections provide a detailed analysis of the second case, highlighting the observed trends, benchmark comparisons with theoretical CJ values, and any notable deviations. These insights will help identify the impact of the modified parameters on wave propagation and combustion performance.

6.2.1 Pressure, Temperature, and Velocity Contours

Figure 6.7 presents the pressure, temperature, and velocity contours for the second case, displayed at intervals of 20 time steps. A clear difference can be observed compared to the first case. The pressure contours show a significant initial pressure spike, reaching a peak value of

8.32E+06 Pa, much higher than the values seen in the first case. This suggests a stronger initial shock at the detonation front, potentially due to a higher energy input or increased reactant availability. However, this pressure spike is followed by a gradual decline, indicating that while the detonation initiates strongly, it begins to dissipate as it propagates.

The temperature contours demonstrate a similar trend, with an initial high-temperature region exceeding 3300 K, followed by a gradual decrease. Notably, the presence of swirling patterns in the temperature field is evident. These swirls suggest localized recirculation zones, which may be a result of boundary interactions, vortex formation, or instability in the post-detonation flow.

The velocity contours exhibit an initial velocity spike, exceeding 1000 m/s, but this rapidly decreases as the wave moves downstream. Similar to the temperature contours, the swirling patterns are visible. These swirls indicate a complex interaction between the detonation wave and the unburned reactants, which may impact wave stability.

Comparing the second case with the first case reveals several key differences. The peak pressure is significantly higher in this case, indicating a stronger initial detonation. However, the presence of swirl patterns suggests potential instability in the post-detonation flow, which was not as prominent in the first case. The higher initial temperature and velocity also suggest a more energetic ignition or enhanced reactant availability.

Overall, the second case demonstrates a more dynamic and potentially unstable detonation behavior, with higher initial energy but also increased instability. Further analysis will be necessary to determine the cause of these swirls and assess their impact on overall performance.

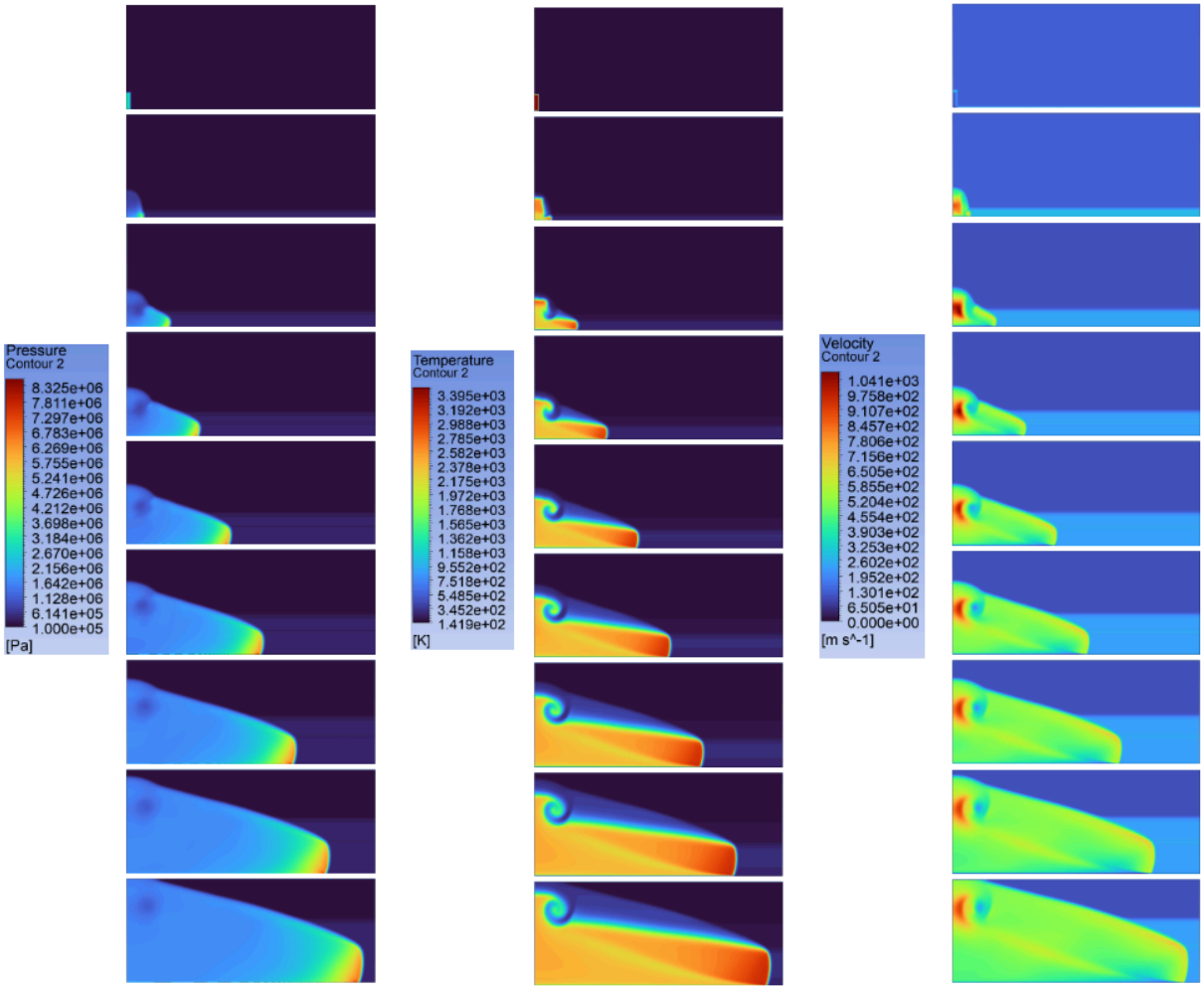

Figure 6.5 - Pressure, temperature, and velocity contour in intervals of 20 time steps.

6.2.2 Analysis of Minimum and Maximum Values

Table 6.3 presents the minimum and maximum values recorded from the pressure, temperature, and velocity contours for the second case. The maximum pressure of 8.96E+06 Pa is significantly higher than the first case, indicating a much stronger initial shock wave. However, the minimum pressure of 100,000 Pa remains consistent with atmospheric conditions, ensuring that the boundary conditions are correctly maintained.

The maximum temperature of 3496.77 K is consistent with the theoretical CJ temperature, demonstrating that the simulation captures the high-energy combustion region accurately. The minimum temperature of 141.85 K is noticeably lower than expected, which may suggest cooling effects or unintended interactions near the boundaries, same as in the first case.

Velocity values range from 0 to 1073.38 m/s, with the maximum velocity approaching the theoretical CJ velocity of 1089.2 m/s. This improvement in velocity suggests that the second case

achieves a more accurate representation of the detonation wave speed, though slight deviations remain.

Table 6.3 - Minimum and maximum values recorded from contours.

Minimum Pressure (Pa)	Maximum Pressure (Pa)	Minimum Temperature (K)	Maximum Temperature (K)	Minimum Velocity (m/s)	Maximum Velocity (m/s)
100000	8.95819E+06	141.851	3496.77	0	1073.38

6.2.3. Experimental CJ Parameters

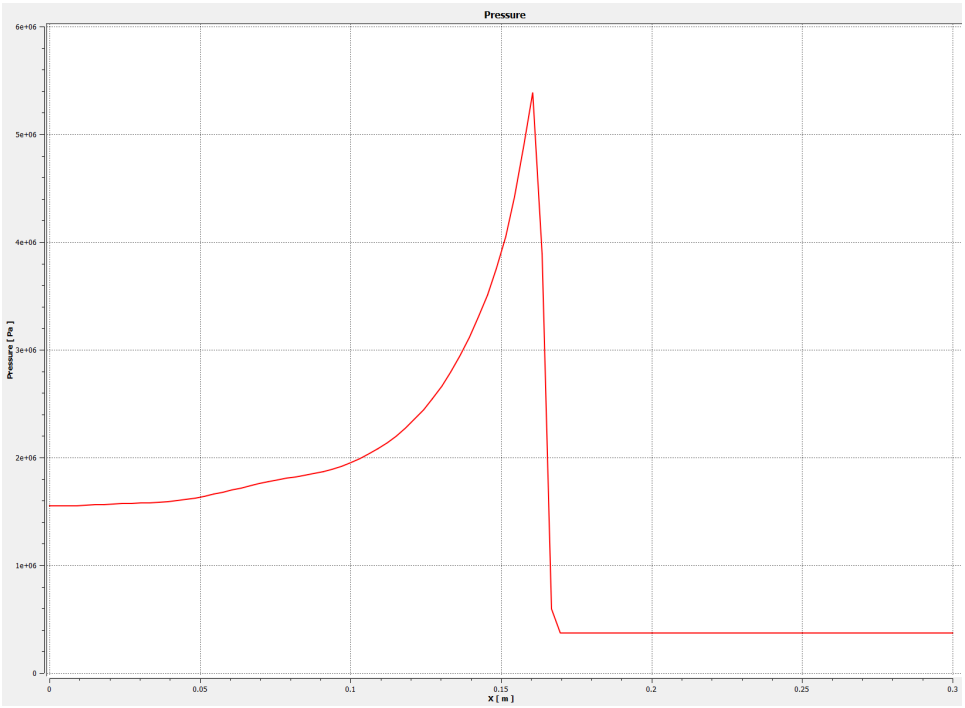

Figure 6.6 - CJ Pressure plot.

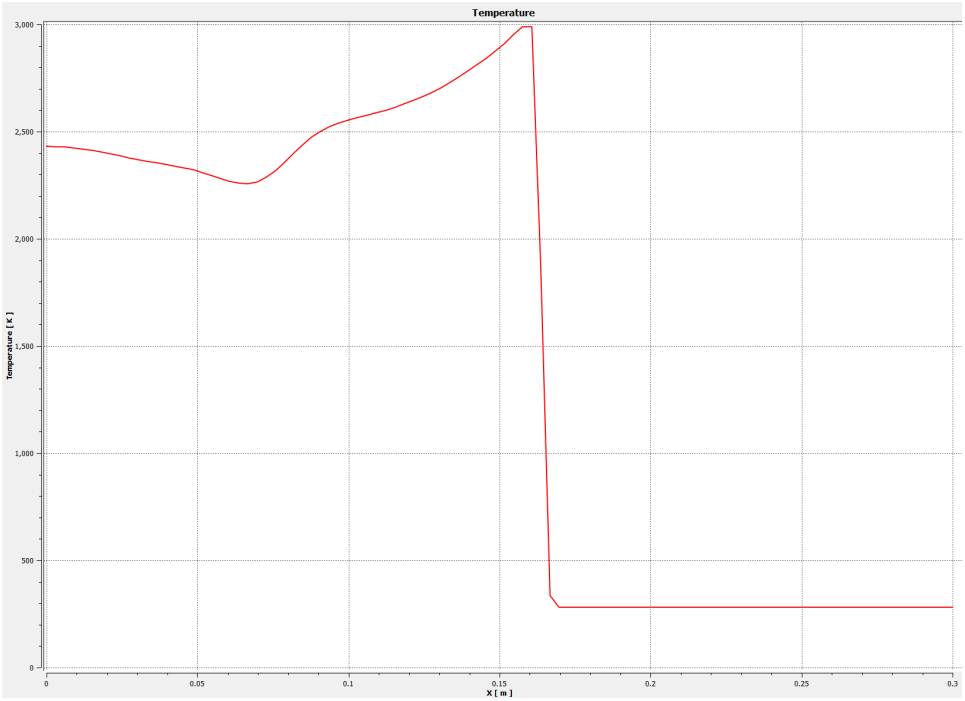

Figure 6.7 - CJ Temperature plot.

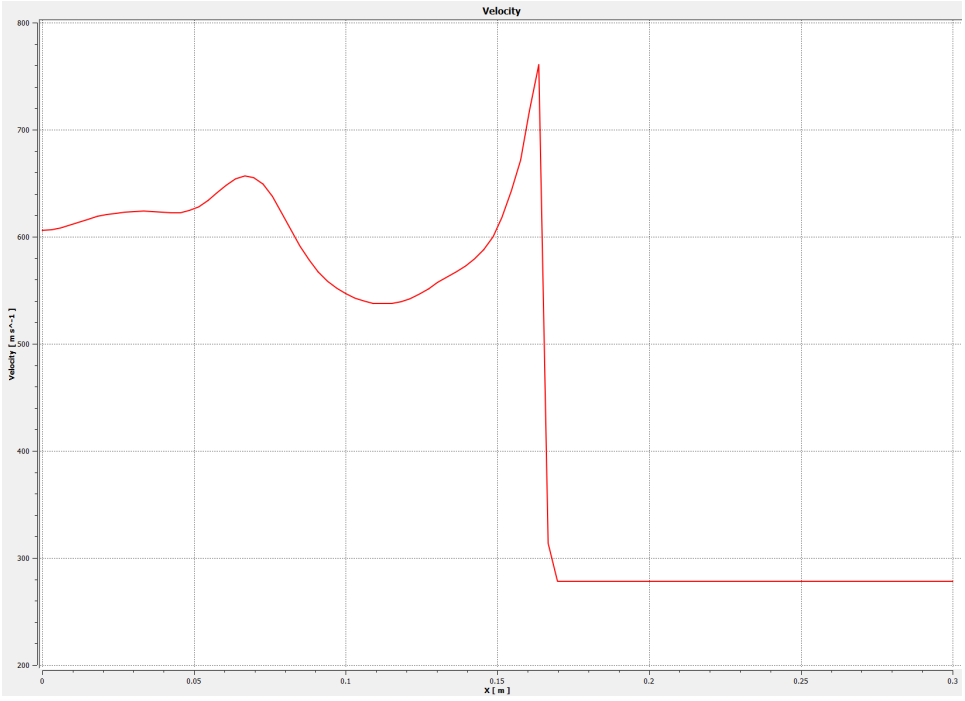

Figure 6.8 - CJ Velocity plot.

Table 6.4 presents a benchmark comparison between the simulation results and the theoretical CJ values obtained from NASA CEA for the second case. The experimental CJ temperature of 2998 K closely aligns with the theoretical value of 2943.85 K, resulting in a minimal percent error of 1.81%. This agreement confirms that the simulation effectively captures the high-temperature characteristics of the detonation wave. However, the experimental CJ pressure of 5,400,000 Pa is significantly higher than the theoretical value of 1,569,600 Pa, leading to a substantial percent error of 256.78%. This extreme deviation suggests that the simulated pressure is experiencing an excessive initial spike, likely due to the strong ignition energy or pressure buildup near the ignition region. The experimental CJ velocity of 760 m/s is noticeably lower than the theoretical value of 1,089.2 m/s, resulting in a percent error of 43.36%. This lower velocity may indicate wave dissipation, insufficient reactant supply, or boundary condition effects that reduce the wave speed.

These benchmark comparisons highlight that while the second case simulation effectively captures the temperature characteristics of the detonation wave, it significantly overestimates pressure and underestimates velocity. These results suggest that further optimization of the ignition model, boundary conditions, and mass flow configuration is required to achieve a more accurate representation of the detonation wave.

Table 6.4 - Benchmark comparison to experimental data.

Experimental CJ Temperature (K)	Theoretical CJ Temperature (K)	Percent Error %	Experimental CJ Pressure (Pa)	Theoretical CJ Pressure (Pa)	Percent Error %	Experimental CJ Velocity (m/s)	Theoretical CJ Velocity (m/s)	Percent Error %
2998	2943.85	1.81%	5,400,000	1,569,600	256.78%	760	1089.2	43.36%

6.3 Discussion

The results and discussion section provided a comprehensive analysis of two simulation cases, each evaluated in terms of pressure, temperature, and velocity contours, as well as benchmark comparisons with theoretical CJ values from NASA CEA. The first case revealed a relatively stable detonation wave with moderate deviations from theoretical values, but also exhibited wave dissipation over time. The second case demonstrated a much stronger initial shock, with higher peak pressures and temperatures but also showed notable swirl patterns, indicating localized instabilities in the flow.

These results highlight several potential areas for improvement. First, the ignition region may require a higher initial energy or an extended size to ensure robust detonation initiation. Second, the mass flow inlet conditions could be adjusted to provide a higher reactant supply, ensuring that the wave remains fueled. Finally, the boundary conditions may need further refinement, such as implementing periodic boundaries or exploring UDF-controlled inlets to maintain a consistent wave structure without dissipation.

Overall, the results demonstrated that while the simulations successfully generated and sustained a certain wave, further improvements are required to enhance accuracy. Specifically, the ignition model, boundary conditions, and mass flow configuration must be optimized to minimize pressure overestimation and improve wave stability. These insights will directly inform the next steps of this research, guiding the refinement of the simulation setup to achieve a more accurate representation of rotating detonation engine behavior.

6.4 Calculation Constraints and Performance Analysis Goals

Despite the extensive analysis conducted on the two simulation cases, the accuracy of the extracted data has proven insufficient for completing the intended performance calculations. Specifically, the pressure, temperature, and velocity data extracted from the simulation are subject to significant deviations from theoretical values, leading to unreliable results for performance metrics such as thrust, specific impulse, and thrust power. Without accurate data, any further analysis using these metrics would lack credibility.

Under ideal conditions, the key performance metrics of the RDE would have been calculated directly from the simulation results. Thrust would be determined based on the product of mass flow rate and exhaust velocity, corrected by the pressure differential between the exit and ambient conditions. Specific impulse would provide a measure of the engine's fuel efficiency, calculated as the thrust divided by the product of mass flow rate and gravitational acceleration. Finally, thrust power would represent the kinetic energy imparted to the exhaust, calculated using the mass flow rate and the square of exhaust velocity. These metrics are essential for assessing the engine's overall performance and comparing it to conventional rocket engines.

$$F = \dot{m}V_e + (P_e - P_{atm})A_e \tag{6.1}$$

$$P_{thrust} = F \times V_e \tag{6.2}$$

$$I_{sp} = V_{eq}/g_o \tag{6.3}$$

Moving forward, it is essential to refine the simulation setup to obtain more accurate pressure, temperature, and velocity data. This includes optimizing the ignition model, adjusting the mass flow conditions, and refining boundary conditions to maintain wave stability. Once reliable data is obtained, these performance calculations can be completed, providing a clear assessment of the RDE's efficiency compared to traditional rocket engines.

Chapter 7: Conclusion and Future Work

This study conducted a comprehensive analysis and literature review of worldwide studies conducted on rotating detonation engine simulations, including a comparative analysis to determine best yielding characteristics. The fundamental principles of detonation, including the background and theory of RDEs were also investigated to provide a fundamental framework and structure to further understand the critical concepts of detonation waves. A custom Python code integrated with Cantera was developed to evaluate and compare the thermodynamic properties of multiple fuel and oxidizer combinations, ensuring the selection of optimal reactants for the RDE configuration. NASA CEA code was then utilized to obtain theoretical CJ values for the selected fuel-oxidizer pair, hydrogen and air, providing a benchmark for evaluating simulation results. An additional focused literature review was conducted on two-dimensional RDE simulations, allowing for a clear understanding of the modeling approaches, boundary conditions, and numerical methods commonly used in similar studies.

The simulation analysis included two cases, each evaluated in terms of pressure, temperature, and velocity characteristics. The first case demonstrated a relatively stable combustion wave with moderate deviations from theoretical CJ values but exhibited wave dissipation over time. In contrast, the second case produced a much stronger initial shock, with higher peak pressures and temperatures, but also displayed significant swirl patterns, indicating potential instability in the post-combustion flow. Despite these differences, both cases effectively captured the high-temperature characteristics of a detonation wave, confirming that the combustion model accurately represented the thermal dynamics of the process.

Benchmark comparisons with NASA CEA theoretical values highlighted notable discrepancies in pressure and velocity. The experimental pressures in both cases significantly exceeded the theoretical CJ values, suggesting over-pressurization caused by the ignition region. The velocities were consistently lower than expected, indicating potential wave dissipation or insufficient reactant supply.

Future work should focus on improving the simulation setup to achieve more accurate pressure, temperature, and velocity data. This includes refining the ignition region, optimizing mass flow inlet conditions, and exploring advanced boundary configurations such as periodic or UDF-controlled inlets. Additionally, once reliable data is obtained, key performance metrics such as thrust, specific impulse, and thrust power can be calculated to provide a quantitative assessment of the RDE's performance compared to conventional rocket engines.

Overall, this study provides a detailed foundation for understanding the behavior of rotating detonation waves in a 2D configuration and highlights critical areas for improvement in the simulation approach. By addressing the identified limitations, future research can achieve a more

accurate and reliable representation of RDE performance, advancing the understanding of this promising propulsion technology.

References

[1] Wolański, P., "Detonative Propulsion," *Proceedings of the Combustion Institute*, Vol. 34, No. 1, 2013, pp. 125–158. https://doi.org/10.1016/j.proci.2012.10.005.

[2] Air Force Research Laboratory, "Rotating Detonation Engines (RDE)," AFResearchLab.com, [Online]. Available: https://afresearchlab.com/technology/rotating-detonation-engines-rde/. [Accessed Nov. 26, 2024]

[3] Teasley, T. W., Fedotowsky, T. M., Gradl, P. R., Austin, B. L., and Heister, S. D., "Current State of NASA Continuously Rotating Detonation Cycle Engine Development," *AIAA SCITECH 2023 Forum*, National Harbor, MD, Jan. 23–27, 2023. https://doi.org/10.2514/6.2023-1873.

[4] Gas Dynamics Imaging Laboratory, "Rotating Detonation Engines," University of Michigan, [Online]. Available: https://gdilab.engin.umich.edu/rotating-detonation-engines/. [Accessed: Feb. 28, 2025].

[5] Voitsekhovsky, B. V., Mitrofanov, V. V., and Topchiyan, M. E., *The Structure of the Detonation Front in Gases*, Publishing House of USSR Academy of Science, Novosibirsk, 1963.

[6] Raytheon Technologies, "More Power, No Moving Parts: Rotating Detonation Engine," RTX.com, Mar. 4, 2025. [Online]. Available: https://www.rtx.com/news/2025/03/04/more-power-no-moving-parts-rotating-detonation-engine. [Accessed: Mar. 24, 2025].

[7] DARPA, "Gambit," Defense Advanced Research Projects Agency, [Online]. Available: https://www.darpa.mil/research/programs/gambit. [Accessed: Mar. 24, 2025].

[8] Venus Aerospace, "Venus Aerospace Rotating Detonation Rocket Engine Achieves Long Duration Run," Venus Aerospace, [Online]. Available: https://www.venusaero.com/venus-aerospace-rotating-detonation-rocket-engine-achieves-long-duration-run/. [Accessed: Mar. 24, 2025].

[9] Venus Aerospace, "VDR2," Venus Aerospace, [Online]. Available: https://www.venusaero.com/vdr2/. [Accessed: Feb. 28, 2025].

[10] Yun, M.-S., Roh, T.-S., and Lee, H. J., "Analysis of Development Trends for Rotating Detonation Engines Based on Experimental Studies," *Aerospace*, Vol. 11, No. 7, 2024, Article 570. https://doi.org/10.3390/aerospace11070570.

[11] Unruh, E., Venters, J., Hemming, M., Lineberry, D., Xu, G., and Frederick, R., "Experimental Study of a Racetrack-Type Rotating Detonation Rocket Engine with Liquid-Fuel Shear-Coaxial Injectors," *AIAA Propulsion and Energy 2021 Forum*, Virtual Event, Aug. 9–11, 2021. https://doi.org/10.2514/6.2021-3683.

[12] Shank, J. C., "Development and Testing of a Rotating Detonation Engine Run on Hydrogen and Air," Master's Thesis, Dept. of Aeronautics and Astronautics, Air Force Institute of Technology, Wright-Patterson AFB, OH, 2012. [Online]. Available: https://scholar.afit.edu/etd/1065.

[13] Anand, V., and Gutmark, E., "Rotating Detonation Combustors and Their Similarities to Rocket Instabilities," *Progress in Energy and Combustion Science*, Vol. 73, 2019, pp. 182–234. https://doi.org/10.1016/j.pecs.2019.04.001.

[14] Tang, X.-M., Wang, J.-P., and Shao, Y.-T., "Three-Dimensional Numerical Investigations of the Rotating Detonation Engine with a Hollow Combustor," *Combustion and Flame*, Vol. 162, No. 4, 2015, pp. 997–1008. https://doi.org/10.1016/j.combustflame.2014.09.023.

[15] Yao, S., Tang, X., Luan, M., and Wang, J., "Numerical Study of Hollow Rotating Detonation Engine with Different Fuel Injection Area Ratios," *Proceedings of the Combustion Institute*, Vol. 36, No. 2, 2017, pp. 2649–2655. https://doi.org/10.1016/j.proci.2016.07.126.

[16] Nakagami, S., Matsuoka, K., Kasahara, J., Matsuo, A., and Funaki, I., "Experimental Study of the Structure of Forward-Tilting Rotating Detonation Waves and Highly Maintained Combustion Chamber Pressure in a Disk-Shaped Combustor," *Proceedings of the Combustion Institute*, Vol. 36, No. 2, 2017, pp. 2673–2680. https://doi.org/10.1016/j.proci.2016.07.097.

[17] Paxson, D. E., "Preliminary Computational Assessment of Disk Rotating Detonation Engine Configurations," *AIAA SciTech 2020 Forum*, Jan. 2020, Orlando, FL

[18] Kawalec, M., and Wolański, P., "Development of Rocket Engine with Continuously Rotating Detonation Supplied by Liquid Propellants," *Proceedings of the 9th European Conference for Aeronautics and Space Sciences*, Lille, France, 27 June 2022.

[19] Kawasaki, A., Inakawa, T., Kasahara, J., Goto, K., Matsuoka, K., Matsuo, A., and Funaki, I., "Critical Condition of Inner Cylinder Radius for Sustaining Rotating Detonation Waves in Rotating Detonation Engine Thruster," *Proceedings of the Combustion Institute*, Vol. 37, No. 3, 2019, pp. 3461–3469. https://doi.org/10.1016/j.proci.2018.07.070.

[20] Nakata, K., Ishihara, K., Goto, K., Itouyama, N., Watanabe, H., Kawasaki, A., Matsuoka, K., Kasahara, J., Matsuo, A., Funaki, I., Higashino, K., Braun, J., Meyer, T., and Paniagua, G., "Experimental Investigation of Inner Flow of a Throatless Diverging Rotating Detonation Engine," *Proceedings of the Combustion Institute*, Vol. 39, No. 3, 2023, pp. 3073–3082. https://doi.org/10.1016/j.proci.2022.08.089.

[21] Zhang, Y., Sheng, Z., Rong, G., Shen, D., Wu, K., and Wang, J., "Experimental Research on the Performance of Hollow and Annular Rotating Detonation Engines with Nozzles," *Applied Thermal Engineering*, Vol. 218, 2023, Article 119339.

[22] Lin, W., Zhou, J., Liu, S., and Lin, Z., "An Experimental Study on CH_4/O_2 Continuously Rotating Detonation Wave in a Hollow Combustion Chamber," *Experimental Thermal and Fluid Science*, Vol. 62, 2015, pp. 122–130. https://doi.org/10.1016/j.expthermflusci.2014.11.017.

[23] Miki, K., Paxson, D. E., Perkins, D., and Yungster, S., "RDE Nozzle Computational Design Methodology Development and Application," *AIAA Propulsion and Energy 2020 Forum*, Virtual Event, August 24–26, 2020. https://doi.org/10.2514/6.2020-3872.

[24] Paxson, D. E., and Schwer, D. A., "Operational Stability Limits in Rotating Detonation Engine Numerical Simulations," AIAA Paper 2019-0748, AIAA SciTech 2019 Forum, San Diego, CA, Jan. 2019.

[25] Paxson, D., "Impact of an Exhaust Throat on Semi-Idealized Rotating Detonation Engine Performance," AIAA Paper 2016-1647, 54th AIAA Aerospace Sciences Meeting, San Diego, CA, Jan. 2016.

[26] Schwer, D., and Kailasanath, K., "Numerical Investigation of the Physics of Rotating-Detonation-Engines," *Proceedings of the Combustion Institute*, Vol. 33, No. 2, 2011, pp. 2195–2202. https://doi.org/10.1016/j.proci.2010.07.050.

[27] Strakey, P. A., Bedick, C. R., and Ferguson, D. H., "Computational Fluid Dynamics Combustion Modeling for Rotating Detonation Engines," U.S. Department of Energy, National Energy Technology Laboratory, Morgantown, WV, and Pittsburgh, PA, 2021. [Online]. Available: https://www.osti.gov/servlets/purl/1765177. [Accessed: Mar. 24, 2025].

[28] Paxson, D., "Pressure-Gain Combustion for Gas Turbines," ASME Turbo Expo 2018: Turbomachinery Technical Conference and Exposition, Oslo, Norway, June 11–15, 2018. NASA John H. Glenn Research Center, Cleveland, OH.

[29] Jiang, Z., and Teng, H., "Gaseous Detonation Physics and Its Universal Framework Theory," in *Proceedings of the International Conference on Aerospace System Science and Engineering 2022*, Springer, Singapore, 2023, pp. 60–62. https://doi.org/10.1007/978-981-19-7002-3.

[30] Wikipedia, “Detonation,” Wikipedia: The Free Encyclopedia, [Online]. Available: https://en.wikipedia.org/wiki/Detonation. [Accessed: Feb. 28, 2025].

[31] [Arthur.N] Nicholls, J. A., Wilkinson, H. R., and Morrison, R. B., “Intermittent Detonation as a Thrust-Producing Mechanism,” Journal of Jet Propulsion, Vol. 27, No. 5, 1957, pp. 534–541. https://doi.org/10.2514/8.12851.

[32] Bulat, P. V., and Volkov, K. N., “The History of the Study of Detonation,” *International Journal of Environmental & Science Education*, Vol. 11, No. 11, 2016, pp. 4894–4909.

[33] Kindracki, J., *Badania Eksperymentalne i Symulacje Numeryczne Procesu Inicjacji Wirującej Detonacji Gazowej*, Ph.D. Dissertation, The Institute of Heat Engineering, 2008.

[34] [Ramamurthi, K., Modeling Explosions and Blast Waves, 2nd ed., Springer, Cham, 2021. https://doi.org/10.1007/978-3-030-74338-3.

[35] Goodwin, D. G., Moffat, H. K., Schoegl, I., Speth, R. L., and Weber, B. W., “Cantera: An Object-Oriented Software Toolkit for Chemical Kinetics, Thermodynamics, and Transport Processes,” Version 3.1.0, 2024. [Online]. Available: https://www.cantera.org. doi:10.5281/zenodo.14455267. [Accessed: Apr. 21, 2025].

[36] NASA Glenn Research Center, “Introduction to CEARUN,” NASA CEARUN, Cleveland, OH, [Online]. Available: https://cearun.grc.nasa.gov/intro.html. [Accessed: Apr. 21, 2025].

[37] NASA Glenn Research Center, Chemical Equilibrium with Applications (CEA) Program, NASA CEARUN, Cleveland, OH, 2018. [Online]. Available: https://cearun.grc.nasa.gov/. [Accessed Apr. 21, 2025].

[38] Raghav, S., Propst, M., Buchholz, M., Tajmar, M., and Bach, C., “Numerical Simulation of 2D Premixed Combustion within a Rotating Detonation Engine,” Proceedings of the ASCenSIon Conference, Dresden, Germany, Sept. 2023.

[39] Benkiewicz, K., “Modeling Two-Dimensional Linear Detonation Engines with ANSYS Fluent Package,” Combustion Engines, 2025. https://doi.org/10.19206/CE-201364.

[40] Borovik, I. N., Farizanov, I. R., and Yanovskii, L. S., “Simulation of Continuous Spin Detonation in an Annular Combustion Chamber in Two-Dimensional Statement,” Thermophysics and Aeromechanics, Vol. 29, No. 1, 2022, pp. 125–142. https://doi.org/10.1134/S0869864322010103.

[41]Paxson, D. E., “Examination of Wave Speed in Rotating Detonation Engines Using Simplified Computational Fluid Dynamics,” AIAA Paper 2018-1883, AIAA SciTech 2018 Forum, Kissimmee, FL, Jan. 8–12, 2018. https://doi.org/10.2514/6.2018-1883.

[42] Farahani, M., and Badrgoltapeh, M., “Two-Dimensional Simulation of Detonation Wave Propagation in a Rotating Detonation Engine,” Proceedings of the 16th International Conference of the Iranian Aerospace Society, Tehran, Iran, Feb. 21–23, 2017.

[43] Wang, F., Liu, Q., and Weng, C., “On the Feasibility and Performance of the Ammonia/Hydrogen/Air Rotating Detonation Engines,” Physics of Fluids, Vol. 35, No. 6, 2023, Paper 066133. https://doi.org/10.1063/5.0152609

[44] Rajak, U., Chaurasiya, P. K., Nashine, P., Kumar, R., and Verma, T. N., “A Numerical Investigation of the Species Transport Approach for Modeling of Gaseous Combustion,” Journal of Thermal Engineering, Vol. 7, Suppl. 14, 2021, pp. 2054–2067. https://doi.org/10.18186/thermal.1051312

[45] Zuniga, S., Investigation of Detonation Theory and the Continuously Rotating Detonation Engine, M.S. Thesis, Dept. of Aerospace Engineering, San José State University, May 2018. [Online]. Available: https://www.sjsu.edu/ae/docs/project-thesis/Samuel.Zuniga-S18_Edited.pdf.

[46] Vaca, I. A., A Systematic Literature Review of Rotating Detonation Engines (RDE’s) & Potential Scalability for Use in Non-Rocket Based Applications, M.S. Thesis, Dept. of Aerospace Engineering, San José State University, May 2023. [Online]. Available: https://www.sjsu.edu/ae/docs/project-thesis/Ian.Vaca-S23.pdf.

Appendix

Appendix A - CJ Calculations and Post Detonation Parameters Calculated Using NASA CEA Code

```
*******************************************************************************
*

      NASA-GLENN CHEMICAL EQUILIBRIUM PROGRAM CEA2, FEBRUARY 5, 2004
            BY  BONNIE MCBRIDE AND SANFORD GORDON
    REFS: NASA RP-1311, PART I, 1994 AND NASA RP-1311, PART II, 1996


*******************************************************************************
*



 ### CEA analysis performed on Mon 21-Apr-2025 16:31:19

 # Problem Type: "Chapman-Jouguet Detonation"

 prob case = _________________8936 det

 # Pressure (1 value):
 p,atm= 1
 # Temperature (1 value):
 t,k= 300

 # Equivalence based on Valence (Eq 9.18*) (1 value):
 r,eq.ratio = 1

 # You selected the following fuels and oxidizers:
 reac
 fuel H2              wt%=100.0000
 oxid Air             wt%=100.0000

 # You selected these options for output:
 # short version of output
```

output short
Proportions of any products will be expressed as Mass Fractions.
output massf
Heat will be expressed as siunits
output siunits
Transport properties calculated
output transport

Input prepared by this script:/var/www/sites/cearun/cgi-bin/CEARUN/prepareInpu
tFile.cgi

IMPORTANT: The following line is the end of your CEA input file!
end

DETONATION PROPERTIES OF AN IDEAL REACTING GAS

CASE = _____

REACTANT		WT FRACTION (SEE NOTE)	ENERGY KJ/KG-MOL	TEMP K
FUEL	H2	1.0000000	0.000	0.000
OXIDANT	Air	1.0000000	0.000	0.000

O/F= 34.29623 %FUEL= 2.833164 R,EQ.RATIO= 1.000000 PHI,EQ.RATIO= 1.000000

UNBURNED GAS

P1, BAR 1.0132
T1, K 300.00
H1, KJ/KG -1.65
M1, (1/n) 21.008
GAMMA1 1.4014
SON VEL1,M/SEC 407.9

BURNED GAS

P, BAR 15.696
T, K 2943.85

RHO, KG/CU M 1.5394 0
H, KJ/KG 1335.47
U, KJ/KG 315.89
G, KJ/KG -29842.8
S, KJ/(KG)(K) 10.5910

M, (1/n) 24.007
(dLV/dLP)t -1.00957
(dLV/dLT)p 1.2069
Cp, KJ/(KG)(K) 3.3589
GAMMAs 1.1636
SON VEL,M/SEC 1089.2

TRANSPORT PROPERTIES (GASES ONLY)
CONDUCTIVITY IN UNITS OF MILLIWATTS/(CM)(K)

VISC,MILLIPOISE 0.98236

WITH EQUILIBRIUM REACTIONS

Cp, KJ/(KG)(K) 3.3589
CONDUCTIVITY 7.7836
PRANDTL NUMBER 0.4239

WITH FROZEN REACTIONS

Cp, KJ/(KG)(K) 1.7716
CONDUCTIVITY 2.8710
PRANDTL NUMBER 0.6062

DETONATION PARAMETERS

P/P1 15.491
T/T1 9.813
M/M1 1.1427
RHO/RHO1 1.8039
DET MACH NUMBER 4.8169
DET VEL,M/SEC 1964.9

MASS FRACTIONS

*Ar 0.01255
*CO 0.00013
*CO2 0.00026
*H 0.00025
HO2 0.00002
*H2 0.00263
H2O 0.22026
*NO 0.00944
NO2 0.00001
*N2 0.72937
*O 0.00136
*OH 0.01356
*O2 0.01014

* THERMODYNAMIC PROPERTIES FITTED TO 20000.K

NOTE. WEIGHT FRACTION OF FUEL IN TOTAL FUELS AND OF OXIDANT IN TOTAL OXIDANTS

Appendix B - Fuel and Oxidizer Thermodynamic Property Calculations Done Using Python Code Integrate with Cantera

```
import numpy as np
import matplotlib as plt
import matplotlib.pyplot as plt
import cantera as ct

def analyze_combustion(fuel, oxidizer, temperature=300, pressure=101325):

    # Gas mixture
    if oxidizer == 'air':
        mixture = f'{fuel}:1, O2:0.21, N2:0.79'
    else:
        mixture = f'{fuel}:1, {oxidizer}:1'

    # Gas object
    gas = ct.Solution('gri30.yaml')  # GRI-Mech 3.0 mechanism

    # Mixture conditions
```

```
    gas.TPX = temperature, pressure, mixture

    # Equilibrate mixture at constant pressure
    gas.equilibrate('HP')

    # Extract thermodynamic properties
    properties = {
        'Temperature (K)': gas.T,
        'Pressure (Pa)': gas.P,
        'Density (kg/m^3)': gas.density,
        'Molar Enthalpy (J/mol)': gas.enthalpy_mass,
        'Molar Entropy (J/mol/K)': gas.entropy_mass,
        'Molar Gibbs Free Energy (J/mol)': gas.gibbs_mass,
        'Molar Heat Capacity (J/mol/K)': gas.cp
    }

    return properties

# Fuel-Oxidizer Combinations
fuels = ['H2', 'CH4', 'C2H6', 'C3H8', 'C2H4']
oxidizers = ['O2', 'air']

# Store results
results = {}

# Analysis of each combination of fuel and oxidizer
for fuel in fuels:
    for oxidizer in oxidizers:
        results[(fuel, oxidizer)] = analyze_combustion(fuel, oxidizer)

# Print Results
for key, value in results.items():
    fuel, oxidizer = key
    print(f"Fuel: {fuel}, Oxidizer: {oxidizer}")
    for prop, val in value.items():
        print(f"  {prop}: {val:.2f}")
    print("\n")
```

Output:
Fuel: H2, Oxidizer: O2

Temperature (K): 2911.27
Pressure (Pa): 101325.00
Density (kg/m^3): 0.09
Molar Enthalpy (J/mol): 3166.91
Molar Entropy (J/mol/K): 13596.62
Molar Gibbs Free Energy (J/mol): -39580245.00
Molar Heat Capacity (J/mol/K): 2244.49

Fuel: H2, Oxidizer: air
Temperature (K): 1938.21
Pressure (Pa): 101325.00
Density (kg/m^3): 0.11
Molar Enthalpy (J/mol): 3511.75
Molar Entropy (J/mol/K): 14042.51
Molar Gibbs Free Energy (J/mol): -27213787.21
Molar Heat Capacity (J/mol/K): 2255.60

Fuel: CH4, Oxidizer: O2
Temperature (K): 2610.67
Pressure (Pa): 101325.00
Density (kg/m^3): 0.07
Molar Enthalpy (J/mol): -1550324.16
Molar Entropy (J/mol/K): 16272.73
Molar Gibbs Free Energy (J/mol): -44033090.59
Molar Heat Capacity (J/mol/K): 2688.90

Fuel: CH4, Oxidizer: air
Temperature (K): 833.00
Pressure (Pa): 101325.00
Density (kg/m^3): 0.28
Molar Enthalpy (J/mol): -1658997.72
Molar Entropy (J/mol/K): 11929.25
Molar Gibbs Free Energy (J/mol): -11596078.82
Molar Heat Capacity (J/mol/K): 2229.88

Fuel: C2H6, Oxidizer: O2

Temperature (K): 1236.74
Pressure (Pa): 101325.00
Density (kg/m^3): 0.12
Molar Enthalpy (J/mol): -1348510.97
Molar Entropy (J/mol/K): 16519.64
Molar Gibbs Free Energy (J/mol): -21779002.34
Molar Heat Capacity (J/mol/K): 2612.10

Fuel: C2H6, Oxidizer: air
Temperature (K): 853.87
Pressure (Pa): 101325.00
Density (kg/m^3): 0.31
Molar Enthalpy (J/mol): -1420532.81
Molar Entropy (J/mol/K): 11166.68
Molar Gibbs Free Energy (J/mol): -10955386.55
Molar Heat Capacity (J/mol/K): 2381.81

Fuel: C3H8, Oxidizer: O2
Temperature (K): 1281.84
Pressure (Pa): 101325.00
Density (kg/m^3): 0.14
Molar Enthalpy (J/mol): -1362277.78
Molar Entropy (J/mol/K): 15156.93
Molar Gibbs Free Energy (J/mol): -20791055.16
Molar Heat Capacity (J/mol/K): 2835.58

Fuel: C3H8, Oxidizer: air
Temperature (K): 589.65
Pressure (Pa): 101325.00
Density (kg/m^3): 0.51
Molar Enthalpy (J/mol): -1421044.62
Molar Entropy (J/mol/K): 9840.40
Molar Gibbs Free Energy (J/mol): -7223482.32
Molar Heat Capacity (J/mol/K): 2085.40

Fuel: C2H4, Oxidizer: O2

Temperature (K): 2330.22
Pressure (Pa): 101325.00
Density (kg/m^3): 0.08
Molar Enthalpy (J/mol): 876466.32
Molar Entropy (J/mol/K): 15694.76
Molar Gibbs Free Energy (J/mol): -35695767.37
Molar Heat Capacity (J/mol/K): 2399.93

Fuel: C2H4, Oxidizer: air
Temperature (K): 1059.24
Pressure (Pa): 101325.00
Density (kg/m^3): 0.28
Molar Enthalpy (J/mol): 924955.01
Molar Entropy (J/mol/K): 10762.77
Molar Gibbs Free Energy (J/mol): -10475412.43
Molar Heat Capacity (J/mol/K): 2254.30